LMSC-HREC TR D867285

(NASA-CR-170875) SPAR IMPROVED
STRUCTURE/FLUID DYNAMIC ANALYSIS CAPABILITY
Interim Report, Aug. 1982 - Aug. 1983
(Lockheed Missiles and Space Co.) 112 p
HC A06/MF A01
CSCL 20D G3/34

N83-36402

Unclas
42200

SPAR
IMPROVED STRUCTURE/FLUID DYNAMIC ANALYSIS CAPABILITY
INTERIM REPORT

August 1983

Contract NAS8-34975

Prepared for

NATIONAL AERONAUTICS AND SPACE ADMINISTRATION
MARSHALL SPACE FLIGHT CENTER, AL 35812

by

J. Tinsley Oden
Mark L. Pearson

Lockheed
Missiles & Space Company, Inc.
Huntsville Research & Engineering Center
4800 Bradford Drive, Huntsville, AL 35807

FOREWORD

This interim report presents the results of work performed under Contract NAS8-34975 for the National Aeronautics and Space Administration, George C. Marshall Space Flight Center, Huntsville, Alabama. This work was performed by personnel in the Product Engineering & Development Section of the Lockheed-Huntsville Research & Engineering Center and by the Computational Mechanics Company, Austin, Texas, subcontractor to Lockheed during this effort.

The period of performance for this study was from August 1982 through August 1983. The MSFC Contracting Officer's Representative for this study is Larry A. Kiefling, ED22.

SUMMARY

This report contains the results of a study whose objective was to add the capability of analyzing a coupled dynamic system of flowing fluid and elastic structure to the SPAR computer code. A comprehensive literature review was performed and a method was developed and adopted for use in SPAR. The method utilizes the existing assumed-stress hybrid Pian element currently in SPAR. An operational module was incorporated in SPAR which provides the capability for analyzing the flow of a two-dimensional, incompressible, viscous fluid within rigid boundaries. Equations were developed to provide for the eventual analysis of the interaction of such fluids with an elastic solid.

CONTENTS

CONTENTS (Concluded)

1. INTRODUCTION

Virtually every structure is in contact with a fluid, be it air, water, or a gas flowing by design or by its natural course over and through the structure's surfaces. The fluid thereby exerts loads on the structure producing deformations which may, in turn, alter the flow of the fluid.

In most situations encountered in the design of engineering systems, this fluid-structure interaction is insignificant, and the structure and the fluid can be analyzed independently. There are important cases, however, in which the interaction of fluid and structural behavior is an intrinsic feature of the response of both media, and this interaction must be taken into account in any rational analysis and design. Such is the case, for example, in the analysis of flutter phenomena in aircraft, the sloshing of fuels or other liquids in flexible tanks, flow-induced vibrations of submerged structures or tall buildings, the safety analysis of nuclear reactor components - particularly the study of pressurized reactor cores - the flow of liquids in flexible pipes as in the flow of blood in elastic arteries or oil or water in rubber hoses, the effects of underwater explosions on submerged structures, etc.

Fluid-structure interaction problems such as these are inherently nonlinear: the domain of fluid media obviously changes with the deformation of the structure and pressures exerted by the fluid act on material surfaces the locations of which depend upon the deformation. There are, however, significant classes of fluid-structure interaction problems for which useful results can be obtained by using only linearized equations. Indeed, the bulk of the work published on this subject deals with one special case or another for which the analyses can be dealt with using linear or mildly nonlinear theories.

In very recent times, important applications have arisen in which a study of rather general and highly nonlinear fluid-structure interaction phenomena is needed. Because of the formidable mathematical difficulties inherent in such nonlinear problems, most analysis procedures in use today are designed for computer implementation. Indeed, for more than two decades, a significant volume of literature on the numerical analysis of fluid-structure interaction problems has accumulated and much of the work over the last decade has involved the development of finite element methods and has primarily focused on problems of nuclear reactor safety.

This report contains a survey and a critical analysis of current numerical schemes used for fluid-structure interaction problems. Special emphasis is placed on finite element methods and on various models and algorithms now in use or under study for a wide class of such problems. We will adopt a deductive approach to this subject, considering first the formulation of very general models for fluid-structure interaction and then reducing these to various special cases that may arise in specific applications.

Following this Introduction, Section 2 contains a brief survey of some of the relevant literature. The principal sources consulted in the preparation of this document are collected in the Bibliography. In Section 3, we discuss so-called mixed Eulerian-Lagrangian descriptions of motion and the corresponding kinematical equations. An attempt is made to present this subject in a relatively thorough and complete way and to provide some clarity and precision in deriving fundamental kinematical relations that are critical to subsequent developments. Derivation of the equations of motion of an arbitrary fluid or solid in such a mixed reference frame is taken up in Section 4. These equations provide the basis for derivation of the semi-discrete systems governing finite-element models of fluid structure interaction, discussed in Sections 5 and 6. Interface conditions are taken up in Section 7. Section 8 contains a derivation of a linear fluid-structure interaction model for nearly incompressible viscous flows. Modifications to the SPAR code to permit incompressible viscous flow calculations are given in Section 9. Results of example problems are presented in Section 10.

2. FINITE ELEMENT METHODS FOR FLUID-STRUCTURE INTERACTION

2.1 GENERAL REMARKS

Interest in the development of finite element methods for fluid-structure interaction problems began primarily in the mid-1970s when concern over the structural integrity of nuclear containment vessels called for better methods for modeling the reactor core, the liquid coolant, surrounding gases and the vessel walls under various conditions. The names Belytschko, Donea, Kennedy, and Liu are prominent in this body of literature, and several surveys of literature on computational methods for fluid-structure interaction in nuclear reactors have been presented by Belytschko and Donea and their associates. In this regard, see, for example, Belytschko (Refs. 1 and 2), Kennedy and Belytschko (Refs. 3 through 5), Belytschko and Kennedy (Refs. 6 and 7), and the references therein to the series of articles by Donea, Fasoli-Stella, and Giuliani (Refs. 8 through 10), Donea, Giuliani, and Halleux (Ref. 11), Donea (Ref. 12), and the dissertation of Liu (Ref. 13). The voluminous collections of proceedings of the biannual SMIRT (Structural Mechanics in Reactor Technology) conferences contain numerous papers on computational methods for fluid-structure interaction problems and there one can find a heavy emphasis on finite element methods.

A significant but relatively smaller collection of papers has been published on finite element methods for flow-induced vibrations of structures, wave effects on submerged structures, and sloshing of liquids in elastic tanks. We shall cite representative examples of this literature later.

2.2 VARIOUS DESCRIPTIONS OF MOTION

The first and most fundamental issue that confronts one in modeling fluid-structure interaction is the choice of an appropriate framework for the description of the motion. Traditionally, in solid mechanics it is natural to adopt a material or Lagrangian description of motion in which the motion of material particles is traced relative to a fixed reference configuration. Thus, one can imagine an actual mass of material, the particles of which are identified (labeled) in some way, and then one proceeds to describe the motion of this mass by giving the spatial positions of each particle relative to a specified (generally fixed) frame of reference at each time, t. Some of the earlier analyses of special classes of fluid-structure interaction problems employed such Lagrangian descriptions, and we mention in this regard the 1980 publication by Kennedy and Belytschko (Ref. 14).

On the other hand, theoretical fluid mechanics traditionally employs a spatial or Eulerian description of motion in which the motion of the fluid through fixed positions in space is characterized as a function of time. Then different fluid (material) particles may occupy the same place in space at different times, and the object is to develop the kinematical description of motion in terms of these places rather than in terms of the particles. Perhaps most of the computational procedures in use for hydrodynamics problems employ an Eulerian description of motion, and some of these have been applied to problems of fluid-structure interaction. See, for example, Chang and Wang (Ref. 15), Harlow and Amsden (Ref. 16), Wang (Ref. 17), Belytschko (Ref. 1), and Dianes, Hirt, and Stein (Ref. 18).

It is clear that in a general fluid-structure interaction problem, neither the Lagrangian/material nor the Eulerian/spatial descriptions are completely satisfactory. It would be fruitless, for example, to attempt to trace the motion of fluid particles in most complex flow phenomena (e.g., stirring of fluid in containers); moreover, the velocity of the fluid at fixed points in its domain is generally the quantity of interest, not the displacement of a particle relative to a fixed point. On the other hand, the motion of a solid through a fluid is most naturally characterized using a material description, but it is this very motion that alters the spatial domain of the fluid with time.

There are also computational advantages and disadvantages inherent in each of these classical descriptions of motion. In the material description, the finite element or finite-difference mesh is imprinted on the material. Thus, with large deformations of the structure, severe distortions of the mesh frequently occur, and this has an adverse effect on the numerical stability, efficiency, and accuracy of most computational procedures. This mesh distortion can be somewhat compensated for by using rezoning techniques wherein new meshes are drawn on the deformed configurations at various time intervals; but these procedures are expensive, difficult to implement, and not completely effective in many situations. The use of an Eulerian scheme to trace both the motion of the fluid and the solid is also imperfect: one must locate material particles of the structure in an Eulerian mesh, and at any particular time the material surfaces of the solid will not, in general, coincide with the spatial grid lines defining the mesh. Some analysts have, nevertheless, attempted to model the geometric changes in the structure with time in an Eulerian description by using a very complex catalogue of material orientations possible in each grid cell (see e.g., Chang and Wang (Ref. 15)). The complexity of such procedures, and of their implementation has discouraged their use in most fluid-structure analysis procedures. One might also mention the presence of convective terms in the momentum equations for Eulerian descriptions of motion. These destroy symmetry in the resulting stiffness equations and lead to many notorious numerical difficulties. While such terms are unavoidable in an Eulerian description of nonuniform fluid flow, their use in the description of the motion of solid bodies can lead to ill-conditioning of the systems of equations governing the discrete model.

2.3 MIXED EULERIAN LAGRANGIAN DESCRIPTIONS

In view of the difficulties noted above, several investigators have attempted to develop mixed Lagrangian Eulerian descriptions of motion, which will be studied in some detail in the Appendix A. These descriptions generally employ, in addition to the spatial and the material frames of reference, a referential or grid system that allows one to displace the finite element mesh so that it is either fixed, in space, moves with the body, or assumes a motion intermediate to these extremes.

The use of a so-called referential frame, distinct from the material and spatial frames of reference, to describe the motion of a continuum can be found in several sources on continuum mechanics. A brief discussion of such systems is given by Truesdell (Ref. 19) in his "Mechanical Foundations of Elasticity and Fluid Mechanics." However, the intent of such developments does not seem to be to provide a basis for studying the interaction of fluids and solids, nor can one find discussions of kinematics of continua sufficiently general to apply directly to interaction problems in any of the standard references on continuum mechanics. Interest in "mixed Eulerian-Lagrangian" descriptions seems to have originated in the computational mechanics literature.

The first attempt at developing computational procedures which employed a mixed Lagrangian-Eulerian description appears to have been in the 1964 papers of Frank and Lazurus (Ref. 20), and Noh (Ref. 21). These authors developed a finite difference scheme for compressible fluid flow in which the motion of the fluid relative to an arbitrary moving grid appears in the governing equations of motion. These formulations attempt to provide for the proper handling of boundary nodes on the fluid-structure interface while allowing nodes interior to the Eulerian mesh to remain fixed and undistorted by the motion of the fluid. Since the resulting formulation retains many features of the Eulerian schemes (e.g. convection like terms), the term quasi-Eulerian is also used to describe them. Another quasi-Eulerian finite difference method was proposed in 1965 by Trulio (Ref. 22) with regard to the AFTON hydrodynamic codes and, a decade after the paper of Frank and Lazarus (Ref. 20), Amsden and Hirt (Ref. 23), of Los Alamos Laboratories, introduced the ALE-technique: Arbitrary Lagrangian-Eulerian (ALE) scheme, which was a finite-difference procedure designed to handle Eulerian and Lagrangian descriptions of motion simultaneously. More recently, finite element codes based on certain aspects of the ALE-strategy have been discussed by Belytschko and Kennedy (Refs. 6 and 7), Belytschko, Kennedy, and Schoeberle (Ref. 24), Donea et al (Refs. 8 and 9), Kennedy and Belytschko (Refs. 3 through 5 and 24), Hughes et al (Ref. 25), Liu (Ref. 13), and Liu and Ma (Ref. 26). These mixed/quasi-Eulerian schemes are not without shortcomings: while they provide for flexibility in descriptions of kinematics and physics, they involve certain features which lead to the necessity of nonconforming finite element methods (see Hughes, Liu, and Zimmerman (Ref. 25)) and the effects of these built-in discontinuities on the accuracy and stability of finite element calculations is, as yet, not known.

In the next section, we shall examine the question of appropriate descriptions of motion in more detail.

3. KINEMATICS OF MOTION AND DEFORMATION

3.1 PRELIMINARIES

In modern continuum mechanics, the study of kinematics of continua generally begins with a mathematical characterization of a continuous body: a body "B" is a differentiable manifold the elements of which are called particles; there is assigned to B a σ-finite Borel measure, called mass of the body. Thus, B is a natural model of a given quantity of matter as a "continuum."

Kinematics aims at describing the motion of B as a function of time. For this purpose, we introduce a time scale $S \in \mathbb{R}$ and measure the motion of B beginning with a fixed instant $\tau = 0$ and over a time interval $\tau \in S = [0,t]$. At each τ, the particles of B are in one-to-one correspondence with points in regions of three-dimensional Euclidian space $E \simeq \mathbb{R}^3$; indeed, the motion of a body implies the existence of bijective (indeed, diffeomorphic) maps $\underset{\sim}{\kappa}_\tau : B \rightarrow \bar{\Omega}_\tau \subset \mathbb{R}^3$ for each time where $\bar{\Omega}_\tau$ is the closure of an open region $\Omega_\tau \subset \mathbb{R}^3$. The regions Ω_τ (or, technically, $\bar{\Omega}_\tau$) are called the configurations of the body.

To give meaning to the maps $\underset{\sim}{\kappa}_\tau$ and to effect a labeling of the particles of B, a particular configuration Ω_R, called the reference configuration, is selected. Typically, $\Omega_R = \Omega_0$, i.e., the reference configuration is the actual region in $\mathbb{R}^3$ occupied by the body at $\tau = 0$, but this is not a necessary choice of the reference configuration. We proceed to introduce in Ω_R a fixed coordinate on $\mathbb{R}^3$ with origin $0 \in \Omega_R$, and we denote by X the position vector of points in Ω_R. In particular, if $\Omega_R = \Omega_{\tau=0}$, and $\underset{\sim}{\kappa} = \underset{\sim}{\kappa}_0$, we set

$$\underset{\sim}{X} = \underset{\sim}{\kappa}(X); \quad \underset{\sim}{\kappa}: B \rightarrow \bar{\Omega}_R \subset \mathbb{R}^3 \tag{3.1}$$

and say that the particle X occupies the position $\underset{\sim}{X}$ in the reference configuration of the body. If X^k, k = 1,2,3, denote the components of $\underset{\sim}{X}$ relative to some fixed basis, then $(X^k) = (X^1, X^2, X^3)$ are referred to as the material coordinates of the particle X.

Physically, the situation can be viewed as this: We wish to name (label) the elements of B, neighborhoods of which can be regarded as actual, physical pieces of matter. To do this, we pick one of the regions in space occupied by the body during its motion, called the reference configuration, and establish in this region a fixed coordinate system $\underset{\sim}{X} \sim (X^k)$. Naturally, since we usually trace the motion of the body from an initial time $\tau = 0$, this reference configuration is ordinarily the actual region occupied by the body at $\tau = 0$. If $\underset{\sim}{X}$ is the position (in space) occupied by the particle $\underset{\sim}{X}$ at $\tau = 0$, then the correspondence $\underset{\sim}{X} = \underset{\sim}{\kappa}(X)$ effectively assigns the numbers (X^1, X^2, X^3) as labels (material coordinates) to the particle X. Thus, X has the same label (X^1, X^2, X^3) for all times $\tau \geq 0$. Since $\underset{\sim}{\kappa}$ is an isometric isomorphism (relative to the usual Euclidean metric), it is usually unnecessary to distinguish between X and its label $\underset{\sim}{X}$ in all subsequent descriptions of the motion of the body B. When the equations of motion of B are written in terms of the material coordinates $\underset{\sim}{X}$, we obtain a material description or Lagrangian* description of motion, as will be further expanded upon below.

*Some argue that this is a misnomer since the equations of motion in terms of the material coordinates were first given by D'Alembert and not Lagrange. See Truesdell (Ref. 19). However, reference to Lagrange here may be due to the analogy of this strategy with that employed by Lagrange in his Mechanique Analytic where he labeled collections of discrete particles and traced their motion relative to a fixed spatial frame of reference. This is essentially what is done here with one fundamental exception: a discrete system has a countable number of particles; thus, natural numbers n N can be used as particle labels. The Body, B, being a continuum, is nondenumerable; thus, a labeling scheme such as the use of triples (X^1, X^2, X^3) of real numbers is needed to label the material particles.

Now, in addition to the material coordinate frame, points in $\mathbb{R}^3$ are identified by the position vectors $\underset{\sim}{x}$ denotes the <u>spatial</u> position occupied by particle $X \varepsilon$ B in a given configuration Ω_t, then there must exist a bijective map $\underset{\sim}{\kappa}_t$: $B \rightarrow \Omega_t$ such that

$$\underset{\sim}{x} = \underset{\sim}{\kappa}_t(X) \tag{3.2}$$

The coordinates (x^k) of $\underset{\sim}{x}$ relative to a given basis are called the <u>spatial coordinates</u> of the particle X at time, t. For each time $\tau \varepsilon S$, there exists a unique configuration Ω_τ of the body, and the family $\{\Omega_\tau\}$ of configurations, dependent on the real parameter, τ, is called the <u>motion</u> of the body. Instead of Eq. (3.1) we describe the motion by a map $\underset{\sim}{\kappa}$: $B \times [0,t] \rightarrow \mathbb{R}^3$ of the form,

$$\underset{\sim}{x} = \nu(X,t) \tag{3.3}$$

Then the curve $\underset{\sim}{x}(t) = \underset{\sim}{\nu}(X,t)$ for finding X, is the path followed by the particle X during the motion of the body. Recalling that $\underset{\sim}{X} = \underset{\sim}{\kappa}(X)$ and that $\underset{\sim}{\kappa}$ is bijective, we can also describe the motion in terms of the material coordinates $\underset{\sim}{X}$:

$$\underset{\sim}{x} = \underset{\sim}{\nu}(X,t) = \underset{\sim}{\nu}(\underset{\sim}{\kappa}^{-1}(\underset{\sim}{X}),t)$$

or

$$x = \chi(\underset{\sim}{X},t) \tag{3.4}$$

where

$$\underset{\sim}{\chi} = \underset{\sim}{\hat{\phi}} \circ \underset{\sim}{\kappa}^{-1} \tag{3.5}$$

Thus, the equation $\underset{\sim}{x} = \underset{\sim}{\chi}(\underset{\sim}{X},t)$ describes the motion of the body relative to the reference configuration in terms of the vectors $\underset{\sim}{X}$ or, equivalently, the material coordinates X^k. When the equations of motion of the body B are written in terms of the spatial positions, $\underset{\sim}{x}$, we obtain a spatial or <u>Eulerian description</u> of the motion. When no confusion is likely, we shall refer to $\underset{\sim}{X}$ and X interchangeably as "a material particle."

The velocity of the material particle $\underset{\sim}{X}$ at time t (relative to $\underset{\sim}{0}$) is the vector

$$\underset{\sim}{v} = \frac{\partial \underset{\sim}{x}\ (\underset{\sim}{X},t)}{\partial t} \tag{3.6}$$

If f is a scalar-values function of particles XϵB, the rate at which f changes in time for fixed X is called the <u>material rate of change</u> of f. We can describe this rate using the <u>material time derivative</u>

$$\frac{Df}{Dt} = \left.\frac{\partial f}{\partial t}\right|_{X \text{ fixed}} \tag{3.7}$$

Thus,

$$\underset{\sim}{v} = D\underset{\sim}{x}/Dt \tag{3.8}$$

If g is given as a function of the spatial coordinates $\underset{\sim}{x} = \chi(\underset{\sim}{X},t)$ of particles X, then

$$\frac{Dg}{Dt} = \frac{\partial g(\underset{\sim}{x},t)}{\partial t} + \frac{\partial g}{\partial x_k}\frac{\partial X_k}{\partial t} \tag{3.9}$$

where x_k denote, for instance, coordinates of $\underset{\sim}{x}$ relative to a fixed basis in $\mathbb{R}^N$ (say Cartesian) and repeated indices are summed, k = 1,2,. . .,N. Thus, if v_k are the corresponding components of $\underset{\sim}{v}$,

$$\frac{Dg}{dt} = \frac{\partial g}{\partial t} + v_k \frac{\partial g}{\partial x_k} \tag{3.10}$$

3.2 THE QUASI-EULERIAN DESCRIPTION

We now set out to derive a description of motion which is sufficiently general to encompass both the material and spatial descriptions as well as intermediate mixed descriptions that may be appropriate for fluid-structure interaction problems. We continue to employ the notations and conventions introduced earlier: for a material body, B, a family of smooth bijective maps $\{\kappa_\tau\}_{0\leq\tau\leq t}$ exist such that

$\underset{\sim}{\kappa}_0$: $B \rightarrow \bar{\Omega} \subset \mathbb{R}^N$, is the reference configuration

$\underset{\sim}{X} = \underset{\sim}{\kappa}_0(X)$ = labels of material particles

= positions of particles in the reference configurations

$\underset{\sim}{\kappa}_t$: $B \rightarrow \Omega_t$ $\mathbb{R}^N$, $\bar{\Omega}_t$ is configuration of the body at time t.

$\underset{\sim}{x} = \underset{\sim}{\kappa}_t (X) = \underset{\sim}{\kappa}_t (\underset{\sim}{\kappa}^{-1} (\underset{\sim}{X}))$ $\chi(\underset{\sim}{X},t)$

= the spatial position of particle X at time t

N = 1, ., or 3.

In addition to these quantities, we introduce a smooth bijective map $\underset{\sim}{\phi}$ from $\hat{\Omega}$ x (0,T) into $\mathbb{R}^N$, such that $\bar{\Omega}_t$ is the image of $\underset{\sim}{\phi}$ at time t:

For $t \varepsilon [0,T]$, $\underset{\sim}{\phi}: \hat{\Omega} \rightarrow \bar{\Omega}_t$ and we write

$$\underset{\sim}{x} = \underset{\sim}{\phi}(\underset{\sim}{y},t) \tag{3.11}$$

or

$$\underset{\sim}{y} = \underset{\sim}{\phi}^{-1} (\underset{\sim}{x},t), \ \underset{\sim}{x} \varepsilon \bar{\Omega}_t, \ t \varepsilon [0,T] \tag{3.12}$$

Since the map $\underset{\sim}{\chi}$ is invertible, we can also write

$$\underset{\sim}{y} = \underset{\sim}{\phi}^{-1} (\underset{\sim}{\chi} (X,t), t) \equiv \underset{\sim}{\psi}(\underset{\sim}{X},t) \tag{3.13}$$

The vectors $\underset{\sim}{y}$ are said to specify <u>referential positions</u> of particles at various times, t. y refers to the position $\underset{\sim}{x}$ of particle $\underset{\sim}{X}$ at time t relative to a moving frame* of reference in $\underset{\sim}{\hat{\Omega}}$ with origin $\underset{\sim}{\hat{0}}$. Thus, we imagine 0

*In this respect, we depart from certain mixed Lagrangian-Eulerian descriptions found in the literature which hold $\hat{\Omega}$ fixed for all times but allow $\Omega(=\Omega_R)$ and Ω_t to be time dependent; see, for example, Hughes et 1 (Ref. 25), Liu (Ref. 13), and Liu and Ma (Ref. 26).

moving with time through space and $\tilde{y} = \tilde{\psi}(\tilde{x},t)$ a vector from $\hat{\tilde{0}}$ to the spatial positions $\tilde{x}$ of particles. We also introduce coordinates X^k, x^k, y^k, k = 1, ..., N, relative to fixed set of basic vectors in each of the respective domains. These notations and the geometrical situation are depicted in Fig. 3-1 for the case in which $\tilde{o}$ and $\tilde{O}$ coincide and are fixed in space.

The coordinates y^k are frequently called the grid- or mesh-coordinates, for reasons which will become clearer later. It is worth noting here, however, that if we lay a fixed mesh on $\hat{\Omega}$, the choice $\tilde{y} \equiv \tilde{X}$ (i.e., $\tilde{\psi} = \tilde{I}$ = the identity) yields a Lagrangian grid whereas the choice $\tilde{y} = x$ produces an Eulerian grid.

In addition to the particle velocity field, (Eq. (3.4)), we introduce the grid velocity $\tilde{v}^G$, which is the rate at which a "grid point" y moves from a fixed position $\tilde{x}$ in space; i.e.,

$$v^G = \frac{\partial}{\partial t}\bigg|_{\tilde{y}\ \text{fixed}} x = \frac{\partial \tilde{\psi}(\tilde{y},t)}{\partial t} \tag{3.14}$$

The so-called difference velocity $\tilde{v}^D$, defined by,

$$\tilde{v}^D = \tilde{v} - \tilde{v}^G \tag{3.15}$$

is then the velocity of a material particle relative to the moving grid $\hat{\Omega}$.

As preparation for a major transformation rule pertaining to material derivatives, we establish the following lemma:

Lemma 3.1. Subject to the conventions and assumptions established above.

ORIGINAL PAGE IS
OF POOR QUALITY

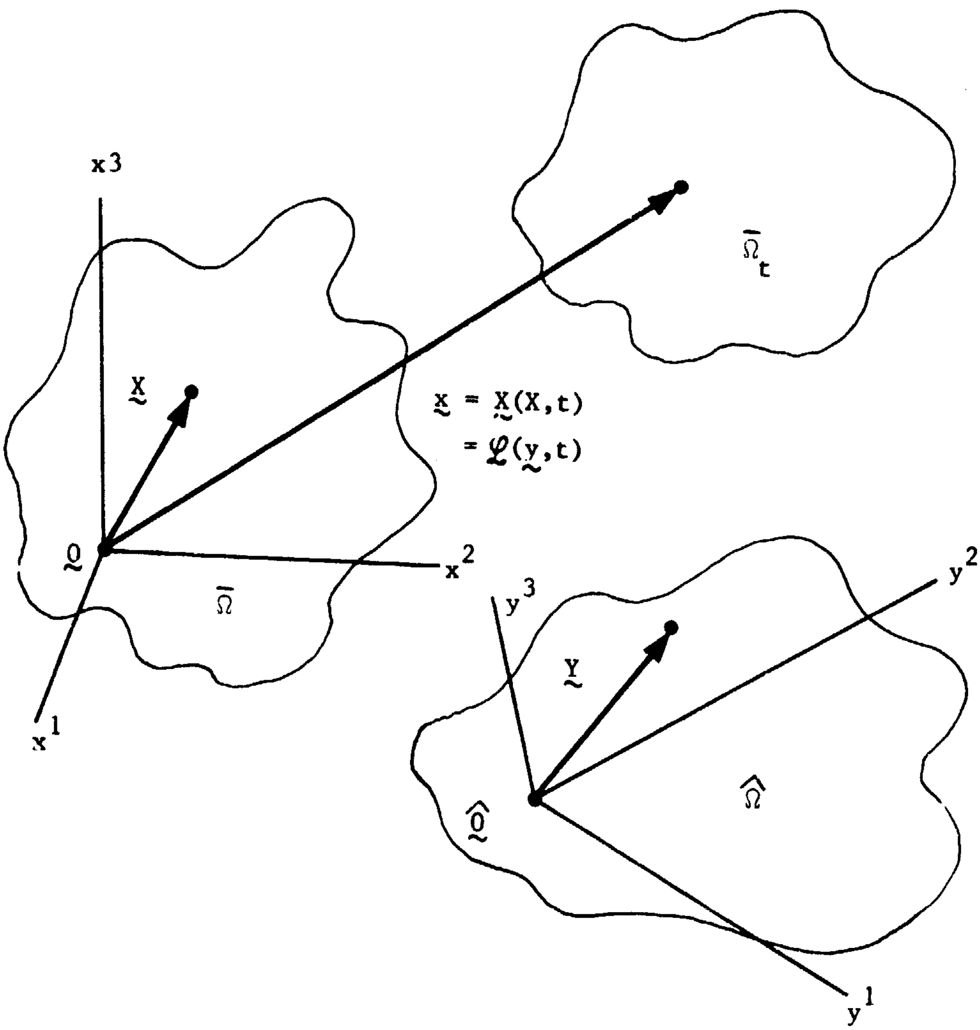

Fig. 3-1 - Various Regions and Coordinate Frames Characterizing the Motion of a Material Body, B

$$\frac{\partial\psi_k^{-1}}{\partial t} = -\frac{\partial\psi_k^{-1}}{\partial x_j} \cdot v_j^G \tag{3.16}$$

where $\underset{\sim}{\psi}^{-1}$ is the inverse of the map $\underset{\sim}{\psi}$ of Eq. (3.11) and the summation convention is used (j, k = 1, 2, ... , N).

<u>Proof:</u> Let y_k denote Cartesian coordinates of $\underset{\sim}{y}$. Then, according to Eq. (3.13),

$$y_k = \psi_k^{-1}(\underset{\sim}{x},t) = \psi_k^{-1}(\psi_j(\underset{\sim}{y},t),t)$$

Differentiating this expression with respect to time holding y_k fixed yields

$$\frac{\partial y_k}{\partial t} = 0 = \frac{\partial\psi_k^{-1}}{\partial x_j} \cdot \frac{j}{t} + \frac{\partial\psi_k^{-1}}{\partial t}$$

as asserted.

Let μ be scalar field given as a differentiable real-values function f of the material coordinates $\underset{\sim}{X}$ and time t:

$$\mu = f(X,t) \tag{3.17}$$

Then the material rate of change of μ is the rate μ changes in time for fixed X:

$$\frac{D\mu}{Dt} = \frac{\partial f(X,t)}{\partial t}$$

The following result allows us to compute the material time derivative of in terms of the grid coordinates and the difference velocity.

<u>Theorem 3.1.</u> Let the conventions established earlier hold and let μ be given by Eq. (3.17). Let

$$\left.\begin{aligned} g(\underset{\sim}{y},t) &= f(\underset{\sim}{\psi}^{-1}(y,t),\ t) \\ h(\underset{\sim}{x},t) &= f(\underset{\sim}{\psi}^{-1}(\underset{\sim}{x},t),\ t) \end{aligned}\right\} \tag{3.18}$$

Then

$$\frac{D\mu}{Dt} = \frac{\partial g(\underset{\sim}{y},t)}{\partial t} + \frac{\partial h(\underset{\sim}{x},t)}{\partial x_j} v_j^D \tag{3.19}$$

<u>Proof:</u> The important idea to be kept in mind here is that we wish to write μ as a function of $\underset{\sim}{y}$ but compute its time-rate-of-change holding $\underset{\sim}{X}$ fixed. We have,

$$\frac{D\mu}{Dt} = \frac{g(\underset{\sim}{y},t)}{\partial t} + \frac{\partial g(\underset{\sim}{\psi}^{-1}(\underset{\sim}{\chi}(\underset{\sim}{X},t),t),t)}{\partial y_k}\left(\frac{\partial \psi_k^{-1}}{\partial x_j}\frac{\partial x_j}{\partial t} + \frac{\partial \psi^{-1}{}_k}{\partial t}\right)$$

But

$$\frac{\partial h(\underset{\sim}{x},t)}{\partial x_j} = \frac{\partial h(\underset{\sim}{\phi}(\underset{\sim}{y},t),t)}{\partial y_k} \cdot \frac{\partial \phi_k^{-1}}{\partial x_j} = \frac{\partial g(\underset{\sim}{y},t)}{\partial y_k} \cdot \frac{\partial \phi_k^{-1}}{\partial x_j}$$

and, from Lemma 1,

$$\frac{\partial g(\underset{\sim}{y},t)}{\partial y_k} \cdot \frac{\partial \phi_k^{-1}}{\partial t} = -\frac{\partial g(\underset{\sim}{y},t)}{\partial y_k} \cdot \frac{\partial \phi_k^{-1}}{\partial x_j} v_j^G = \frac{\partial h(\underset{\sim}{x},t)}{\partial x_j} v_j^G)$$

Thus,

$$\frac{D\mu}{Dt} = \frac{\partial g(\underset{\sim}{y},t)}{t} + \frac{\partial h(\underset{\sim}{x},t)}{x_j}(v_j - v_j^G)$$

as asserted.

It is important to note that Eq. (3.16) reduces to conventional Lagrangian or Eulerian descriptions with appropriate choices of the coordinates y^k or the map $\underset{\sim}{\phi}$:

Lagrangian:

$$\underset{\sim}{\phi} = \underset{\sim}{\chi}, \; \underset{\sim}{v}^G = \frac{\partial \chi(\underset{\sim}{X},t)}{\partial t} = \underset{\sim}{v}, \; \underset{\sim}{v}^D = \underset{\sim}{0}$$

$$\frac{D\mu}{Dt} = \frac{\partial g(\psi(\underset{\sim}{X},t),t)}{\partial t} = \frac{\partial f(\underset{\sim}{X},t)}{\partial t}$$

Eulerian:

$$\underset{\sim}{\phi} = \underset{\sim}{I}, \; \underset{\sim}{v}^G = \frac{\partial}{\partial t}\bigg|_{\underset{\sim}{x}\ \text{fixed}} \underset{\sim}{x} = 0, \; \underset{\sim}{v}^D = \underset{\sim}{v}$$

$$\frac{D\mu}{Dt} = \frac{\partial g(\underset{\sim}{x},t)}{\partial t} + \frac{\partial h(\underset{\sim}{x},t)}{\partial x_i} v_i$$

3.3 OTHER KINEMATICAL EQUATIONS

Some simplifications in the developments can be realized by considering the referential coordinates to coincide with the material coordinates of a particle X at time $\tau = 0$ and to regard the "grid" as moving relative to the reference configuration Ω at an arbitrary velocity $\underset{\sim}{v}^G$ which is not directly dependent on the particles. If X^α, x_k y_k are Cartesian components of $\underset{\sim}{X}$, $\underset{\sim}{x}$, and $\underset{\sim}{y}$ relative to fixed bases, we have

$$y_k = \psi_k\,(\underset{\sim}{X},t), \; v_k^G = \frac{\partial \psi_k}{\partial t} \tag{3.20}$$

Let

$$J(\underset{\sim}{X},t) \equiv \det\left|\frac{\partial y_k}{\partial X^\alpha}\right| \tag{3.21}$$

Then we have the following results:

Lemma 3.2

$$\frac{DJ}{Dt} = J\underset{\sim}{\nabla} \cdot \underset{\sim}{v}^G \equiv J\,\frac{\partial v_k^G}{\partial y_k} \tag{3.22}$$

Proof: Let

$$y_{k,\alpha} = \frac{\partial y_k}{\partial X^\alpha}$$

and let $\varepsilon^{\alpha\beta\gamma}$, ε_{ijk} denote the alternating tensors. Then

$$J = \det[y_{k,\alpha}] = \frac{1}{6}\,\varepsilon^{\alpha\beta\gamma}\,\varepsilon^{ijk}\,y_{i,\alpha}\,y_{j,\beta}\,y_{k,\gamma}$$

and

$$\frac{\partial J}{(y_{r,\theta})} = \frac{1}{2}\,\varepsilon^{\alpha\beta\theta}\,\varepsilon_{ijr}\,y_{i,\alpha}\,y_{j,\beta} \tag{3.23}$$

Since

$$\frac{\partial y_k}{\partial X^\alpha}\cdot\frac{\partial X^\alpha}{\partial y_j} = \delta_{ij}$$

we have

$$\frac{\partial X^\alpha}{\partial y_j} = \frac{\text{cofactor }[y_{k,\alpha}]}{\det\,[y_{k,\alpha}]} = \frac{1}{2J}\,\varepsilon^{\rho\beta\alpha}\,\varepsilon_{kij}\,y_{k,\rho}\,y_{\beta,i} \tag{3.24}$$

Thus, from Eqs. (3.23) and (3.24)

$$\frac{\partial J}{\partial(y_{r,\theta})} = \text{cofactor } y_{r,\theta} = J\,\frac{\partial X^\theta}{\partial y_r} \tag{3.25}$$

Also note that

$$\frac{\partial}{\partial t}\,y_{r,\theta} = \frac{\partial}{\partial X^\theta}\cdot\frac{\partial y_r}{\partial t} = v^G_{r,\theta} \tag{3.26}$$

Thus,

$$\frac{\partial J}{\partial t} = \frac{\partial J}{\partial (y_{r,\theta})} \cdot \frac{\partial y_{r,\theta}}{\partial t}$$

$$= J \frac{\partial X^\theta}{\partial y_r} \cdot \frac{\partial v_r^G}{\partial X^\theta}$$

$$= J \frac{\partial v_f^G}{\partial y_r} = J\nabla \cdot v^G$$

Lemma 3.3. Given a differentiable real-values function $g = g(y,t) = g(\psi(X,t),t)$, we have

$$(1) \qquad \frac{dg}{dt} = \frac{\partial g}{\partial t} + \frac{\partial g}{\partial y_k} v_k^G \tag{3.27}$$

Similarly,

$$(2) \quad \frac{d(g,J)}{dt} = J[\frac{\partial g}{\partial t} + \nabla \cdot (g v^G)] \tag{3.28}$$

Proof: Condition (1) is obvious. To obtain (2), note that

$$\nabla \cdot (gv^G) \equiv \frac{\partial}{\partial y_k} (g(y,t)\ v_k^G(y,t))$$

$$= g\ \nabla \cdot v^G + v^G \cdot \nabla g$$

$$J\nabla \cdot (gv^G) = gJ\nabla \cdot v^G + Jv^G \cdot \nabla g = g \frac{\partial J}{\partial t} + Jv^G \cdot \nabla g \tag{3.29}$$

where we have made use of Lemma 3.2. Thus, from Eqs. (3.27) and 3.29)

$$\frac{d(gJ)}{dt} = \frac{\partial gJ}{\partial t} + v^G \cdot \nabla g$$

$$= J \frac{\partial g}{\partial t} + J \frac{\partial g}{\partial t} + v^G \cdot \nabla g$$

$$= J \frac{\partial g}{\partial t} + J\nabla \cdot (gv^G)$$

is asserted.

We will use these results in the next section to derive equations of motion in the grid (referential) coordinates y_k.

3.4 A SPECIAL REFERENTIAL DESCRIPTION OF MOTION

A fairly general discussion of kinematics in a grid or referential system was given earlier. We will now focus on special extensions and applications of those ideas which lead to a convenient framework for treating practical problems in fluid-structure interaction. The structure of this kinematical description is outlined in the following five steps:

1. Spatial Frame. We establish an absolutely fixed (spatial) Reference frame in $\mathbb{R}^N$; the position vectors $\underset{\sim}{x}$ are defined by their Cartesian components x_k, $1 \leq k \leq N$.

2. Material Frame. At time $t = 0$, a material body B occupies a region $\overline{\Omega} \subset \mathbb{R}^N$ and we use as labels of the particles of B the coordinates, X_k, of their positions in this reference configuration; the corresponding places of particles $\{X_k\}$ are identified by vectors $\underset{\sim}{X}$.

3. Motion. The motion of B is, as usual, defined by the specification of the position $x \in \mathbb{R}^N$ of each particle $\underset{\sim}{X}$ at each time, t, $0 \leq t \leq T$:

$$\underset{\sim}{x} = \underset{\sim}{\chi}(\underset{\sim}{X},t) \tag{3.30}$$

   The motion $\underset{\sim}{\chi}$ is assumed to be a differentiable bijective map from $\overline{\Omega}$ into $\overline{\Omega}$ into $\Omega_t \subset \mathbb{R}^N$ at each time, t.

4. Grid Positions. We introduce an arbitrary, differentiable, injective function ϕ: $\Omega \times [0,T] \to \mathbb{R}^3 \times [0,T]$, such that for each $\tilde{t} \in [0,T]$, the range of $\underset{\sim}{\phi}$ is a region $\hat{\Omega}_t \subset \mathbb{R}^3$. The "position" vectors

$$\underset{\sim}{y} = \phi(\underset{\sim}{X},t), \qquad \underset{\sim}{y} \in \hat{\Omega}_t \tag{3.31}$$

   are said to define the grid positions in $\mathbb{R}^N$. Note that $\underset{\sim}{y}$ is a position vector of a point (place) in $\mathbb{R}^N$. These positions depend only indirectly on the locations $\underset{\sim}{x}$ of material particals, viz,

$$\underset{\sim}{y} = \underset{\sim}{\phi}(\underset{\sim}{\chi}^{-1}(\underset{\sim}{x},t),t) = \underset{\sim}{\psi}(\underset{\sim}{x},t) \tag{3.32}$$

5. Displacements and Velocities. One can define the particle displacement u and the particle velocity, $\underset{\sim}{v}$, by

$$\left.\begin{aligned} \underset{\sim}{u}(\underset{\sim}{X},t) &= \underset{\sim}{x} - \underset{\sim}{X} \equiv \underset{\sim}{\chi}(\underset{\sim}{X},t) - \underset{\sim}{X} \\ \underset{\sim}{v}(\underset{\sim}{X},t) &= \frac{D\underset{\sim}{x}}{Dt} = \frac{\partial \underset{\sim}{\chi}(\underset{\sim}{X},t)}{\partial t} \end{aligned}\right\} \tag{3.33}$$

and the grid displacement u^G and grid velocity v^G by

$$\left.\begin{aligned} \underset{\sim}{u}^G(\underset{\sim}{X},t) &= \underset{\sim}{y} - \underset{\sim}{X} = \underset{\sim}{\phi}(\underset{\sim}{X},t) - \underset{\sim}{X} \\ \underset{\sim}{v}^G(\underset{\sim}{X},t) &= \frac{\partial \underset{\sim}{\phi}(\underset{\sim}{X},t)}{\partial t} = \left.\frac{\partial \underset{\sim}{y}}{\partial t}\right|_{X \text{ fixed}} \end{aligned}\right\} \tag{3.34}$$

These quantities and notations are illustrated in Fig. 3-1.

3.5 JACOBIANS AND TIME RATES

Let y_k, X_α denote components of $\underset{\sim}{y}$ and $\underset{\sim}{X}$ relative to a fixed basis. We denote by j the Jacobian of the transformation $\underset{\sim}{X} \mapsto \underset{\sim}{\phi}(\underset{\sim}{X},t)$ for each t:

$$j(\underset{\sim}{X},t) = \det\left|\frac{\partial y_k}{\partial X_\alpha}\right| = \det\left|\frac{\partial \phi_k(\underset{\sim}{X},t)}{\partial X_\alpha}\right| \tag{3.35a}$$

Likewise, we denote

$$J(X,t) = \det\left|\frac{\partial x_k}{\partial X_\alpha}\right| = \det \frac{\partial \phi_k(\underset{\sim}{X},t)}{\partial X_\alpha} \tag{3.35b}$$

Then, as was proved in Section 3.3,

$$\boxed{\begin{aligned} \frac{\partial j}{\partial t} &= j\,\frac{\partial v_k^G}{\partial y_k} = j\,\underset{\sim}{\nabla}\cdot\underset{\sim}{v}^G \\ \frac{\partial J}{\partial t} &= J\,\frac{\partial v_k}{\partial x_k} = J\,\underset{\sim}{\nabla}\cdot\underset{\sim}{v} \end{aligned}} \tag{3.36}$$

Note that the operator ∇ is the same spatial gradient operator in both of these expressions owing to our definition of y_k. In both expressions, the time-rate-of-change is taken with $\underset{\sim}{X}$ fixed.

Next, we let g denote values of a given real-valued function of particles and time, and introduce the notations

$$\begin{aligned} g &= \text{value of field at particle } \underset{\sim}{X} \text{ at time } t \\ &= \bar{g}(\underset{\sim}{X},t) = \tilde{g}(\underset{\sim}{x},t) = \hat{g}(\underset{\sim}{y},t) \end{aligned} \tag{3.37}$$

where

$$\left.\begin{aligned} \tilde{g}(\underset{\sim}{x},t) &= \bar{g}(\underset{\sim}{\chi}^{-1}(\underset{\sim}{x},t),t) \\ \hat{g}(\underset{\sim}{y},t) &= \bar{g}(\underset{\sim}{\phi}^{-1}(\underset{\sim}{y},t),t) \end{aligned}\right\} \tag{3.38}$$

$$\boxed{\begin{aligned} \frac{Dg}{Dt} &= \text{material time-derivative of } g \\ &= \text{time-rate-of-change of } g \text{ for fixed particle } \underset{\sim}{X} \\ &= \frac{\partial \bar{g}}{\partial t} \\ &= \frac{\partial \tilde{g}}{\partial t} + \underset{\sim}{v} \cdot \underset{\sim}{\nabla}\tilde{g} \\ &= \frac{\partial \hat{g}}{\partial t} + \underset{\sim}{v}^G \cdot \underset{\sim}{\nabla}\tilde{g} \end{aligned}} \tag{3.39}$$

where it is understood that

$$\frac{\partial \hat{g}}{\partial t} = \text{the time-rate-of-change of } g \text{ holding the spatial position } \underset{\sim}{y} \text{ fixed.} \tag{3.40}$$

ORIGINAL PAGE IS
OF POOR QUALITY

Thus, while the forms of the functions $\tilde{g}$ and $\hat{g}$ may be different, the partials $\partial\tilde{g}/\partial t$ and $\partial\hat{g}/\partial t$ both represent the rate g changes in t at a fixed spatial position.

Combining the above results, we arrive at the equations

$$\boxed{\begin{aligned} \left.\frac{\partial(jg)}{\partial t}\right|_{\underset{\sim}{X}\text{ fixed}} &= \frac{\partial(jg)}{\partial t} \\ &= \bar{j}\left(\frac{\partial\hat{g}}{\partial t} + \underset{\sim}{\nabla} \cdot \underset{\sim}{v}^{G}\hat{g}\right) \\ \left.\frac{\partial(Jg)}{\partial t}\right|_{\underset{\sim}{X}\text{ fixed}} &= \frac{\partial\overline{Jg}}{\partial t} \\ &= \bar{J}\left(\frac{\partial\tilde{g}}{\partial t} + \underset{\sim}{\nabla} \cdot \underset{\sim}{v}\tilde{g}\right) \end{aligned}} \tag{3.41}$$

Also note that

$$\left.\begin{aligned} \left.\frac{\partial(jg)}{\partial t}\right|_{\underset{\sim}{X}\text{ fixed}} &= j\left(\frac{\partial\tilde{g}}{\partial t} + \underset{\sim}{v} \cdot \underset{\sim}{\nabla}\tilde{g} + \tilde{g}\underset{\sim}{\nabla} \cdot \underset{\sim}{v}^{G}\right) \\ \left.\frac{\partial(Jg)}{\partial t}\right|_{\underset{\sim}{X}\text{ fixed}} &= J\left(\frac{\partial\hat{g}}{\partial t} + \underset{\sim}{v}^{G} \cdot \underset{\sim}{\nabla}\hat{g} + g\underset{\sim}{\nabla} \cdot \underset{\sim}{v}\right. \end{aligned}\right\} \tag{3.42}$$

We now make a fundamental observation*: the partial derivatives $\partial\hat{g}/\partial t$ and $\partial\tilde{g}/\partial t$ represent time-rates-of-change at fixed points in space. The values of these rates coincide if we take $\underset{\sim}{\phi} = \underset{\sim}{\chi}$ and $\underset{\sim}{v}^{G} = 0$. Thus,

*This observation was apparently first made by Donea et al (Ref. 10); see also Donea (Ref. 12) and Belytschko and Kennedy (Ref. 27).

$$\boxed{\left.\frac{\partial g(\underset{\sim}{\chi}(\underset{\sim}{X},t),t)}{\partial t}\right|_{\substack{\underset{\sim}{X}_G=\underset{\sim}{\phi} \\ \underset{\sim}{v}=0}} = \frac{\partial g(\underset{\sim}{\phi}(\underset{\sim}{X},t),t)}{\partial t}} \qquad (3.43)$$

This relationship proves to be crucial in deriving local equations of motion in referential coordinates since it enables us to transform any standard Eulerian form (spatial time rates) into a corresponding time derivative in grid coordinates. We will exploit this idea in Section 4.

4. EQUATIONS OF MOTION

4.1 INTRODUCTORY REMARKS

We consider the motion of a material body subjected to body forces of intensity, $\underset{\sim}{b}$, per unit mass and surface tractions, $\underset{\sim}{S}$, on a portion, $\partial\Omega_2$, of its boundary. We focus our attention on control volumes $\tilde{\Omega} \subset \mathbb{R}^N$ with boundary $\overline{\partial\tilde{\Omega} = \partial\tilde{\Omega}_1 \cup \partial\tilde{\Omega}_2}$, the velocities being prescribed on $\partial\tilde{\Omega}_1$ and the tractions on $\partial\tilde{\Omega}_2$. Alternatively, to obtain equations of motion in referential coordinates, we consider a control volume, $\hat{\Omega}_t = \phi(\Omega,t)$, moving with the grid velocity, $\underset{\sim}{v}^G$, and with boundaries, $\overline{\partial\hat{\Omega} = \partial\hat{\Omega}_1 \cup \partial\hat{\Omega}_2}$. Components of vectors are referred to a fixed orthonormal basis characterizing the spatial coordinates, x_k. Indicial notation and the summation convention are used in some of the relationships which follow. The following additional notations are introduced:

ρ = the value of the mass density of the body in the current configuration,

$$\rho = \tilde{\rho}(\underset{\sim}{x},t) = \hat{\rho}(\underset{\sim}{\chi}(\underset{\sim}{X},t),t) = \bar{\rho}(\underset{\sim}{X},t)$$

$\underset{\approx}{\sigma}$ = the Cauchy stress tensor, with Cartesian components relative to spatial coordinate directions of

$$\sigma_{ij} = \tilde{\sigma}_{ij}(\underset{\sim}{x},t) = \hat{\sigma}_{ij}(\underset{\sim}{\chi}(\underset{\sim}{x},t),t) = \bar{\sigma}_{ij}(\underset{\sim}{X},t)$$

$\underset{\sim}{b}$ = the body force vector per unit mass in the current configuration with Cartesian components

$$b_i = \tilde{b}_i(\underset{\sim}{x},t) = \hat{b}_i(\underset{\sim}{\chi}(\underset{\sim}{X},t),t) = \bar{b}_i(\underset{\sim}{X},t)$$

ε = the internal energy per unit mass in the current configuration of the body, defined by functions

$$\varepsilon = \tilde{\varepsilon}(\underset{\sim}{x},t) = \hat{\varepsilon}(\underset{\sim}{\chi}(\underset{\sim}{X},t),t) = \bar{\varepsilon}(\underset{\sim}{X},t)$$

Other notations will be introduced later.

4.2 LOCAL EULERIAN FORMS

The local Eulerian (spatial) forms of the equations of motion of an arbitrary continuum are:

1. Conservation of Mass

$$\frac{\partial \rho}{\partial t} + \underset{\sim}{\nabla} \cdot (\tilde{\rho} \underset{\sim}{v}) = 0 \tag{4.1}$$

2. Balance of Linear Momentum

$$\frac{\partial \tilde{\rho} \tilde{v}_k}{\partial t} + \frac{\partial}{\partial x_i} (\tilde{\rho} \tilde{v}_i \tilde{v}_k) = \tilde{\rho} \tilde{b}_k + \frac{\partial \tilde{\sigma}_{ki}}{\partial x_i} \tag{4.2}$$

3. Balance of Angular Momentum

$$\tilde{\sigma}_{ij} = \tilde{\sigma}_{ji} \tag{4.3}$$

4. Conservation of Energy

$$\frac{\partial \tilde{\rho} \tilde{E}}{\partial t} + \frac{\partial}{\partial x_i} (\tilde{\rho} \tilde{v}_i \tilde{E}) = \tilde{\rho} \tilde{b}_i \tilde{v} + \frac{\partial \tilde{\sigma}_{ik} \tilde{v}_k}{x_i} + \tilde{Q} \tag{4.4}$$

where

$\tilde{E}$ = total energy per unit mass

$$= \frac{1}{2} \underset{\sim}{v} \cdot \underset{\sim}{v} + \varepsilon \tag{4.5}$$

$\tilde{Q}$ = heat working

$$= \frac{\partial \tilde{q}_i}{\partial x_i} + \tilde{\rho} \tilde{r} \tag{4.6}$$

and q_i are the components of the heat flux vector and r is the heat supplied per unit mass per unit time in the current configuration. For simplicity, we will take $\tilde{Q} = Q$ in subsequent developments; but it should be clear that the addition of Q and thermal effects produced no significant complications in any of the following developments.

4.3 LOCAL REFERENTIAL FORMS

A direct application of relations (3.41) and (3.43) derived in the previous section and the above Eulerian forms leads to local equations of motion in the grid-coordinates, y_k.

The superposed caret (^) denotes functions of the referential coordinates y_k and time. Thus, for example, the mass density is given by

$$\rho = \hat{\rho}(\underset{\sim}{y},t)$$

where it is understood that

$$\begin{aligned} \hat{\rho}(\underset{\sim}{y},t) &= \hat{\rho}(\underset{\sim}{\phi}(X,t),t) \\ &= \bar{\rho}(\underset{\sim}{X},t) = \tilde{\rho}(\underset{\sim}{x},t) \end{aligned} \tag{4.7}$$

etc.,

1. <u>Conservation of Mass.</u> In view of Eq. (3.41a),

$$\left.\frac{\partial \widehat{j\rho}}{\partial t}\right|_X = j\left(\frac{\partial\hat{\rho}}{\partial t} + \underset{\sim}{\nabla} \cdot \hat{\rho}\underset{\sim}{v}^G\right)$$

where $|_X$ indicates that the time derivative is taken with $\underset{\sim}{X}$ held fixed. But, according to Eqs. (3.43) and (4.1),

$$\frac{\partial\rho(\underset{\sim}{y},t)}{\partial t} = \left.\frac{\partial\rho(\underset{\sim}{\chi}(\underset{\sim}{X},t),t)}{\partial t}\right|_{\substack{\underset{\sim}{X}_G=\underset{\sim}{\phi} \\ \underset{\sim}{v}^G=\underset{\sim}{0}}} = -\underset{\sim}{\nabla} \cdot \hat{\rho}\underset{\sim}{v}$$

Thus,

$$\left.\frac{\partial \widehat{j\rho}}{\partial t}\right|_{\underset{\sim}{X}} = j\underset{\sim}{\nabla} \cdot \hat{\rho}\underset{\sim}{v}^D \tag{4.8}$$

where $\underset{\sim}{v}^D$ is, again the difference velocity

$$\underset{\sim}{v}^D = \underset{\sim}{v}^G - \underset{\sim}{v} \tag{4.9}$$

Alternatively, since

$$\left.\frac{\partial j\hat{\rho}}{\partial t}\right|_{\underset{\sim}{X}} = \hat{\rho}\,\frac{\partial j}{\partial t} + j\,\frac{\partial\hat{\rho}}{\partial t} \qquad (\underset{\sim}{X}\text{ fixed})$$

$$= \hat{\rho} j \underset{\sim}{\nabla} \cdot \underset{\sim}{v}^G + j \left.\frac{\partial\hat{\rho}}{\partial t}\right|_{\underset{\sim}{X}}$$

we have

$$\left.\frac{\partial\hat{\rho}}{\partial t}\right|_{\underset{\sim}{X}} = -\hat{\rho}\nabla \cdot v^G + v_k^D\,\frac{\partial\hat{\rho}}{\partial y_k} + \rho\underset{\sim}{\nabla} \cdot (\underset{\sim}{v}^G - \underset{\sim}{v})$$

or

$$\left.\frac{\partial\hat{\rho}}{\partial t}\right|_{\underset{\sim}{X}} = \underset{\sim}{v}^D \cdot \underset{\sim}{\nabla}\hat{\rho} - \hat{\rho}\underset{\sim}{\nabla} \cdot \underset{\sim}{v} \tag{4.10}$$

2. <u>Balance of Linear Momentum.</u> Let

$$\hat{p}_i = \hat{\rho}\hat{b}_i + \frac{\partial\hat{\sigma}_{ki}}{\partial y_k} \tag{4.11}$$

Then a calculation similar to that leading to Eq. (4.8) yields the momentum equation in referential form,

$$\left.\frac{\partial\widehat{\rho j v_k}}{\partial t}\right|_{\underset{\sim}{X}} = j\,\frac{\partial}{\partial y_i}\,(\hat{\rho}\hat{v}_k\,\hat{v}_i^D) + j\hat{p}_k \tag{4.12}$$

Similarly, by expanding the left-hand side of this equation and using Eq. (3.41), we have the equivalent equations,

$$\hat{\rho}\left.\frac{\partial \hat{v}_i}{\partial t}\right|_{\underset{\sim}{X}} = \hat{\rho} v_k^D \frac{\partial v_i}{\partial y_k} + p_i - v_i \left[\left.\frac{\partial \widehat{\rho j}}{\partial t}\right|_{\underset{\sim}{X}} - j\frac{\partial}{\partial y_k}(\hat{\rho} v_k^D)\right] \tag{4.13}$$

According to Eq. (4.8), the term in brackets vanishes if mass is constant locally.

3. Balance of Angular Momentum. Denoting

$$\begin{aligned} \hat{\sigma}_{ij}(\underset{\sim}{y},t) &= \hat{\sigma}_{ij}(\underset{\sim}{\phi}(\underset{\sim}{X},t),t) \\ &= \bar{\sigma}_{ij}(\underset{\sim}{X},t) \\ &= \bar{\sigma}_{ij}(\underset{\sim}{\chi}^{-1}(\underset{\sim}{x},t),t) \\ &= \tilde{\sigma}_{ij}(\underset{\sim}{x},t) \end{aligned} \tag{4.14}$$

angular momentum is balanced locally if

$$\hat{\sigma}_{ij}(\underset{\sim}{y},t) = \hat{\sigma}_{ji}(\underset{\sim}{y},t) \tag{4.15}$$

4. Conservation of Energy. By following the identical process used to obtain Eqs. (4.8) and (4.12), we arrive at the following referential form of the conservation of energy,

$$\begin{aligned} \left.\frac{\partial \widehat{j\rho E}}{\partial t}\right|_{\underset{\sim}{X}} &= j\left(\frac{\partial \widehat{\rho E}}{\partial t} + \underset{\sim}{\nabla}\cdot \hat{\rho}\hat{E}\underset{\sim}{v}^G\right) \\ &= j\Big[\hat{\rho}\hat{b}_k\hat{v}_k + \frac{\partial}{\partial y_k}(\hat{\sigma}_{ik}v_i) \\ &\quad + \frac{\partial}{\partial y_k}(\hat{\rho}\hat{E}\hat{v}_k^D)\Big] \end{aligned} \tag{4.16}$$

Since $E = 1/2\, v^2 + \varepsilon$ ($v^2 = \underset{\sim}{v} \cdot \underset{\sim}{v}$), we can also write this result in the form

$$\left.\frac{\partial(j\widehat{\rho\varepsilon})}{\partial t}\right|_{\underset{\sim}{X}} = j\frac{\partial}{\partial y_k}(\hat{\rho}\hat{\varepsilon}v_k^D) + j\hat{\sigma}_{ik}\frac{\partial v_k}{\partial y_i}$$

$$- \frac{v^2}{2}\underset{\sim\sim\sim\sim\sim\sim\sim\sim\sim\sim}{\left[\left.\frac{\partial j\hat{\rho}}{\partial t}\right|_{\underset{\sim}{X}} - j\frac{\partial\hat{\rho}v_k^D}{y_k}\right]}$$

$$- jv_k\underset{\approx\approx\approx\approx\approx\approx\approx\approx\approx\approx\approx\approx\approx\approx\approx\approx\approx}{\left[\hat{\rho}\left.\frac{\partial\hat{v}_k}{\partial t}\right|_{\underset{\sim}{X}} - \hat{\rho}v_j^D\frac{\partial v_k}{\partial y_j} - \hat{\rho}b_k - \frac{\partial\hat{\sigma}_{ik}}{\partial y_i}\right]} \qquad (4.17)$$

If mass is conserved, the term with a single wavy underline vanishes, by virtue of Eq. (4.8). Likewise, the term with double wavy underlines reduces then to the local momentum equation (Eq. 4.13) which also vanishes. Then if linear momentum is balanced, we have

$$\left.\frac{\partial(j\widehat{\rho\varepsilon})}{\partial t}\right|_{\underset{\sim}{X}} = j\frac{\partial}{\partial y_k}(\hat{\rho}\hat{\varepsilon}v_k^D) + j\,\hat{\sigma}_{ik}\frac{\partial v_k}{\partial y_k} \qquad (4.18)$$

Finally, since

$$\left.\frac{\partial j\widehat{\rho\varepsilon}}{\partial t}\right|_X = j\left.\frac{\partial\rho\varepsilon}{\partial t}\right|_X + \rho\varepsilon j\underset{\sim}{\nabla}\cdot\underset{\sim}{v}^G$$

we have

$$\left.\frac{\partial\widehat{\rho\varepsilon}}{\partial t}\right|_X = \hat{\sigma}_{ki}\frac{\partial\hat{v}_k}{\partial y_i} + v_k^D\frac{\partial\hat{\rho}\hat{\varepsilon}}{\partial y_k} - \rho\hat{\varepsilon}\frac{\partial\hat{v}_k}{\partial y_k} \qquad (4.19)$$

5. Summary. In summary, the local equations of motion in referential form are given by

$$
\boxed{
\begin{aligned}
\frac{\partial\hat{\rho}}{\partial t} &= \hat{\underset{\sim}{v}}^D \cdot \underset{\sim}{\nabla}\hat{\rho} - \hat{\rho}\underset{\sim}{\nabla} \cdot \hat{\underset{\sim}{v}} \\
\frac{\partial\hat{v}_i}{\partial t} &= \hat{\rho}v_k^D \frac{\partial\hat{v}_i}{\partial y_k} + \hat{\rho}\hat{b}_i + \frac{\partial\hat{\sigma}_{ki}}{\partial y_k} \\
\hat{\sigma}_{ij} &= \hat{\sigma}_{ji} \\
\frac{\partial\widehat{\rho\varepsilon}}{\partial} &= \hat{v}_k^D \frac{\partial\widehat{\rho\varepsilon}}{\partial y_k} - \hat{\rho}\hat{\varepsilon}\frac{\partial\hat{v}_k}{\partial y_k} + \hat{\sigma}_{ki}\frac{\partial\hat{v}_k}{\partial y_i} \\
& 1 \le i,j,k \le N;\ N = 1,2,\text{ or } 3
\end{aligned}
}
\tag{4.20}
$$

wherein it is understood that the time-derivatives on the left side of the equality are computed holding $\underset{\sim}{X}$ fixed and that the quantities appearing on the right side are regarded as functions of the grid coordinates, y_k.

4.4 GLOBAL FORMS

Let $d\hat{v}$ be a differential volume element in $\hat{\Omega}_t$ and $d\hat{s}$ an element of surface area of the boundary, $\partial\hat{\Omega}_t$, with unit exterior normal, $\hat{\underset{\sim}{n}}$. The control referential volume, $\hat{\Omega}_t$, is moving with the grid velocity, $\underset{\sim}{v}^G$, relative to the fixed spatial frame of reference as before. Let dv_o denote a material volume element in the reference configuration, so that

$$
d\hat{v} = \left| \det \frac{\partial y_i}{\partial X_\alpha} \right| du_o = j dv_o
$$

Finally, let G be a quantity to be conserved in a physical process and supposed G is given by

$$
G(t) = \int_{\hat{\Omega}_t} \hat{g}(\underset{\sim}{y},t)\, d\hat{v}
$$

Then the time-rate-of-change of G is

$$\frac{dG(t)}{dt} = \frac{\partial}{\partial t} \int_{\hat{\Omega}_t} \hat{g}(\underset{\sim}{y},t)\, d\hat{v}$$

$$= \frac{\partial}{\partial t} \int_{\Omega} \hat{g}(\underset{\sim}{\phi}(\underset{\sim}{X},t),t)j\, dv_o$$

$$= \int_{\Omega} \frac{\partial \hat{g} j}{\partial t}\, dv_o$$

$$= \int_{\Omega} (\frac{\partial \hat{g}}{\partial t}) + \underset{\sim}{\nabla} \cdot \underset{\sim}{v}^G \hat{g})j\, dv_o$$

$$= \int_{\hat{\Omega}_t} \frac{\partial \hat{g}}{\partial t}\, d\hat{v} + \int_{\hat{\Omega}_t} \underset{\sim}{\nabla} \cdot \underset{\sim}{v}^G g\, d\hat{v}$$

Hence, an application of the divergence theorem yields

$$\frac{dG(t)}{dt} = \int_{\hat{\Omega}_t} \frac{\partial \hat{g}}{\partial t}\, d\hat{v} + \int_{\partial\hat{\Omega}} \underset{\sim}{v}^G \cdot \hat{\underset{\sim}{n}}\, g\, d\hat{s} \tag{4.21}$$

1. Mass. Since

$$\frac{\partial \hat{\rho}}{\partial t} = - \underset{\sim}{\nabla} \cdot \hat{\rho} v$$

$$\int_{\hat{\Omega}_t} \frac{\partial \hat{\rho}}{\partial t}\, d\hat{v} = - \int_{\partial\hat{\Omega}_t} \hat{\rho}\hat{\underset{\sim}{v}} \cdot \hat{\underset{\sim}{n}}\, d\hat{s} \tag{4.22}$$

Hence, if M(t) is the total mass of $\hat{\Omega}_t$ at time, t,

$$\frac{dM(t)}{dt} = \frac{d}{dt} \int_{\hat{\Omega}_t} \hat{\rho}\, d\hat{v} = \int_{\partial\hat{\Omega}_t} \hat{\rho}\underset{\sim}{v}^D \cdot \hat{\underset{\sim}{n}}\, d\hat{s} \tag{4.23}$$

2. Linear Momentum. If $\underset{\sim}{P}(t)$ is the total linear momentum of $\hat{\Omega}_t$ at time, t, then an application of Eq. (4.21) yields for the global form of the rate-of-change of $\underset{\sim}{P}$,

$$\frac{dP(t)}{dt} = \frac{d}{dt} \int_{\hat{\Omega}_t} \hat{\rho}\hat{v}\, d\hat{v}$$

$$= \int_{\partial\hat{\Omega}_t} \rho \underset{\sim}{v} (\underset{\sim}{v}^G \cdot \hat{\underset{\sim}{n}})\, d\hat{s}$$

$$+ \int_{\hat{\Omega}_t} (\mathrm{div}\, \hat{\underset{\approx}{\sigma}} + \hat{\rho}\hat{\underset{\sim}{b}})\, d\hat{v} \tag{4.24}$$

3. __Energy.__ Likewise, the rate-of-change of total energy is

$$\frac{d\varepsilon(t)}{dt} = \frac{d}{dt} \int_{\hat{\Omega}_t} \hat{\rho}\hat{E}\, d\hat{v} = \int_{\hat{\Omega}_t} \hat{\rho}\hat{b} \cdot \hat{v}\, d\hat{v} + \int_{\partial\hat{\Omega}_t} (\hat{\rho}\hat{E}\, \underset{\sim}{v}^D \cdot \hat{\underset{\sim}{n}}$$

$$+ \hat{\underset{\sim}{s}} \cdot \hat{\underset{\sim}{v}})\, d\hat{s} \tag{4.25}$$

5. VARIATIONAL PRINCIPLES

5.1 SPACES OF ADMISSIBLE FIELDS

We shall introduce abstract linear spaces of admissible densities, velocities, and internal energy: Let $\hat{\Omega}$ denote a "control volume" in the referential system moving with a velocity field, $\underset{\sim}{v}^G$, relative to the fixed spatial frame and let $\partial\hat{\Omega}$ denote its boundary. The boundary, $\partial\hat{\Omega}$, is further decomposed into portions, $\partial\hat{\Omega}_1$, and $\partial\hat{\Omega}_2$ where the velocities $\underset{\sim}{v}$, $\underset{\sim}{v}^G$ and the tractions $\hat{s}_k = \hat{\sigma}_{ki}n_i$ are prescribed, respectively, $\underset{\sim}{\hat{n}}$ being a unit normal to $\partial\hat{\Omega}$. We have thus, for each $t \in [0,T]$, $\hat{\Omega} = (\underset{\sim}{\phi},t)$

Let

$\underset{\sim}{V}$ = space of admissible velocities

$$= \left\{ \underset{\sim}{v} \,\middle|\, \left| \int_{\hat{\Omega}} \hat{\sigma}_{ki}(\underset{\sim}{v}) \frac{\partial v_k}{\partial y_i} d\hat{v} \right| < \infty, \quad \underset{\sim}{v} = \underset{\sim}{0} \text{ on } \partial\hat{\Omega}_1 \right\} \tag{5.1}$$

R = space of admissible densities

$$= \left\{ \phi \,\middle|\, \left| \int_{\hat{\Omega}} (\underset{\sim}{v}^D \cdot \phi\underset{\sim}{\nabla}\phi + \phi \frac{\partial\phi}{\partial t}) d\hat{v} \right| < \infty \;\forall t \in [0,T] \right\} \tag{5.2}$$

E = space of admissible internal energy densities

$$= \left\{ \psi \,\middle|\, \left| \int_{\hat{\Omega}} (\psi\sigma_{ki} \frac{\partial v_k}{\partial y_k} + \phi\psi\underset{\sim}{\nabla} \cdot \underset{\sim}{v} + \psi\underset{\sim}{v}^D \cdot \underset{\sim}{\nabla}\phi\psi) d\hat{v} \right| < \infty, \quad \forall\phi\in R, \forall v \in V, \forall t \in [0,T] \right\} \tag{5.3}$$

At this stage, these spaces are too vaguely defined to have important mathematical significance. More specific properties of these spaces can be established once constitutive equations for the material have been defined. Typically, the spaces $\underset{\sim}{V}$, R, and E will be Orlicz-Sobolev spaces such as $R = W^{s,p}(\Omega, L^q(0,T))$, etc. We shall give more concrete definitions of these spaces in later developments.

5.2 VARIATIONAL PROBLEM IN REFERENTIAL FORM

We now consider the following variational problem:

Given body forces f, grid velocity field v^G, and tractions $\underset{\sim}{S}$ on $\partial\hat{\Omega}_2$, find a triple $(\rho, \underset{\sim}{u}, \varepsilon) \in R \times \underset{\sim}{V} \times E$ such that

$$\int_{\hat{\Omega}} \left(\frac{\partial\rho}{\partial t}\phi + \phi\rho\underset{\sim}{\nabla}\cdot\underset{\sim}{u}\right) d\hat{v} = \int_{\hat{\Omega}} \underset{\sim}{v}^D \cdot \underset{\sim}{\nabla}\rho\phi \, dv$$

$$\int_{\hat{\Omega}} (\rho\underset{\sim}{v}) \cdot \frac{\partial\underset{\sim}{u}}{\partial t} - \rho v_i v_k^D \frac{\partial u_i}{\partial y_k}) \, d\hat{v}$$

$$= \int_{\hat{\Omega}} \left(\sigma_{ki}\frac{\partial v_k}{\partial y_i} + \rho b_i \hat{v}_i\right) dv + \int_{\partial\hat{\Omega}_2} S_i \, v_i \, d\hat{s} \tag{5.4}$$

$$\int_{\hat{\Omega}} \left(\psi\frac{\partial\rho\varepsilon}{\partial t} + \psi\rho\varepsilon\frac{\partial u_k}{\partial y_k} - \psi \, v_k^D \frac{\partial\rho\varepsilon}{\partial y_k} - \sigma_{ki}\frac{\partial u_k}{\partial y_k}\psi\right) d\hat{v} = 0$$

$$\forall(\phi, \underset{\sim}{v}, \psi) \in R \times \underset{\sim}{V} \times E$$

It is easily shown that any solution of the equations of motion (4.20) is also a solution of the variational Eqs. (5.4). Conversely, any sufficiently smooth solution of Eq. (5.4) is at least a weak solution of Eq. (4.20). Thus, Eqs. (5.4) represent a set of variational equations equivalent to the equations of motion in referential form.

6. FINITE ELEMENT MODELS

6.1 THE DISCRETE VARIATIONAL PROBLEM

The construction of finite element models of the general fluid-structure interaction problem embodied in Eqs. (5.4) follows the standard steps:

1. The domain, $\hat{\Omega}$, is partitioned into E finite elements such that for each $t \in [0,T]$

$$\hat{\Omega} = \bigcup_{e} \bar{\Omega}_e, \quad \Omega_e \cap \Omega_f = \phi \quad e = f$$

2. Piecewise polynomial shape functions are defined over each element which rpovide a basis for local approximations of ρ, $\underset{\sim}{u}$, and ε. Typically, these have the properties

$$\rho_h^e = \sum_{N=1}^{R_e} \rho_e^N(t)\, \beta_N^e(y)$$

$$\underset{\sim}{u}_h^e = \sum_{M=1}^{N_e} \underset{\sim}{u}_e^M(t)\, \phi_M^e(\underset{\sim}{y}) \tag{6.1}$$

$$\varepsilon_h^e = \sum_{L=1}^{K_e} \varepsilon_e^L(t)\, \psi_L^e(\underset{\sim}{y})$$

where R_e, N_e, and K_e denote the numbers of element-degrees-of-freedom for the respective local approximations; ρ_e^N, $\underset{\sim}{u}_e^M$, and ε_e^L denote nodal values of ρ_h^e, $\underset{\sim}{u}_h^e$, and ε_h^e at time t, and the local shape functions usually satisfy conditions of the type

$$\left.\begin{array}{lll} \beta_N^e(\underset{\sim}{y}_\rho^M) = \delta_N^M, & 1 \le M, N \le R_e \\ \phi_M^e(\underset{\sim}{y}_u^N) = \delta_N^M, & 1 \le M, N \le N_e \\ \psi_L^e(\underset{\sim}{y}_\varepsilon^N) = \delta_L^M, & 1 \le L, N \le K_e \end{array}\right\} \tag{6.2}$$

with $\underset{\sim}{y}_\rho^N$, $\underset{\sim}{y}_u^N$, and $\underset{\sim}{y}_\varepsilon^N$ the element coordinates of nodes corresponding to the local approximations of ρ, $\underset{\sim}{u}$, and ε, respectively.

3. The shape functions are designed so that they match at inter-element boundaries so as to produce global basis functions

$$B_i(\underset{\sim}{y}),\ \Phi_j(\underset{\sim}{y}),\ \Psi_k(\underset{\sim}{y})\ (1 \le i \le R,\ 1 \le j \le N,\ 1 \le k \le K),$$

which are defined over the entire domain $\hat{\Omega}$ and which provide basic functions for finite-dimensional spaces R^h, $\underset{\sim}{V}^h$, and E^h, respectively, and so that

$$B_i\Big|_{\overline{\Omega}_e} = \beta_N^e,\ \Phi_j\Big|_{\overline{\Omega}_e} = \phi_N^e,\ \Psi_k\Big|_{\Omega_e} = \psi_N^e \tag{6.3}$$

In conforming finite element approximations, frequently have

$$R^h \subset R,\ \underset{\sim}{V}^h \subset \underset{\sim}{V},\ E^h \subset E \tag{6.4}$$

where R, $\underset{\sim}{V}$, and E are the spaces of admissible functions introduced in the previous secton. We shall not, however, restrict our analyses to conforming finite elements.

6.2 SEMI-DISCRETE MODEL

The semi-discrete, Galerkin, finite element approximation of the variational problem (Eq. (5.4)) is characterized by the following discrete problem:

$$
\left.
\begin{aligned}
&\text{Given } \underset{\sim}{f},\ \underset{\sim}{v}^G, \text{ and } \underset{\sim}{S}, \text{ find } (\rho_h, \underset{\sim}{u}_h, \varepsilon_h) \in R^h, \underset{\sim}{V}^h, E^h \text{ such that}\\
&\int_{\hat{\Omega}} \left(\phi_h \frac{\partial \rho_h}{\partial t} + \phi_h \rho_h \underset{\sim}{\nabla} \cdot \underset{\sim}{u}_h\right) d\hat{v} = \int_{\hat{\Omega}} \underset{\sim}{v}_h^D \cdot \underset{\sim}{\nabla} \rho_h^1 \phi_h \, d\hat{v}\\
&\int_{\hat{\Omega}} \left(\rho_h \underset{\sim}{v}_h \cdot \frac{\partial \underset{\sim}{u}_h}{\partial t} - \rho_h v_i^h v_{hk}^D \frac{\partial u_{hi}}{\partial y_k}\right) d\hat{v}\\
&= \int_{\hat{\Omega}} \left(\sigma_{ki} \frac{\partial v_{hi}}{\partial y_i} + \rho_h b_i V_{hi}\right) d\hat{v} + \int_{\partial\Omega_2} S_i v_{hi} \, d\hat{s}\\
&\int_{\hat{\Omega}} \left(\psi_h \frac{\partial \rho_h \varepsilon_h}{\partial t} + \psi_h \rho_h \varepsilon_h \frac{\partial u_{hk}}{\partial y_k} - \psi_h v_{hk}^D \frac{\partial \rho_h \varepsilon_h}{\partial y_k}\right.\\
&\qquad\qquad \left. -\sigma_{ki} \frac{\partial u_{hk}}{\partial y_k} \psi_h\right) d\hat{v} = 0\\
&\qquad \forall (\phi_h, \underset{\sim}{v}_h, \psi_h) \in R^h \times V^h \times E^h
\end{aligned}
\right\}
\qquad (6.5)
$$

where

$$\underset{\sim}{v}_h^D = \underset{\sim}{v}^G - \underset{\sim}{v}_h.$$

7. INTERFACE CONDITIONS

The main difficulty in employing a general ALE-type description of motion for fluid-structure interaction problems is the specification of boundary conditions at the interface of Eulerian and Lagrangian meshes and at free boundaries. If Γ denotes any material surface on which such conditions are to be imposed, then a necessary condition to be met is

$$v^G = v_n \quad \text{on } \Gamma \tag{7.1}$$

where $v^G = \underset{\sim}{v}^G \cdot \underset{\sim}{n}$, $v_n = \underset{\sim}{v} \cdot \underset{\sim}{n}$, and

$\underset{\sim}{v}^G$ = the grid velocity
$\underset{\sim}{v}$ = the particle velocity
$\underset{\sim}{n}$ = a unit normal to Γ

To generalize this condition, consider the situation shown in Fig. 7-1 in which a nodal point N is assigned a given trajectory and velocity $\underset{\sim}{v}^G$. The material surface, Γ, is assumed to be given by the equation

$$x_2 = \phi(x_1) \text{ or } x_1 = \psi(x_2)$$

If

$\underset{\sim}{i}_1$ = unit orthonormal basis vectors

$\underset{\sim}{r}$ = position vector of points on surface Γ

then

$$\underset{\sim}{n} = \frac{1}{\sqrt{1 + \phi'^2}} \left[\phi' \underset{\sim}{i}_1 - \underset{\sim}{i}_2\right]$$

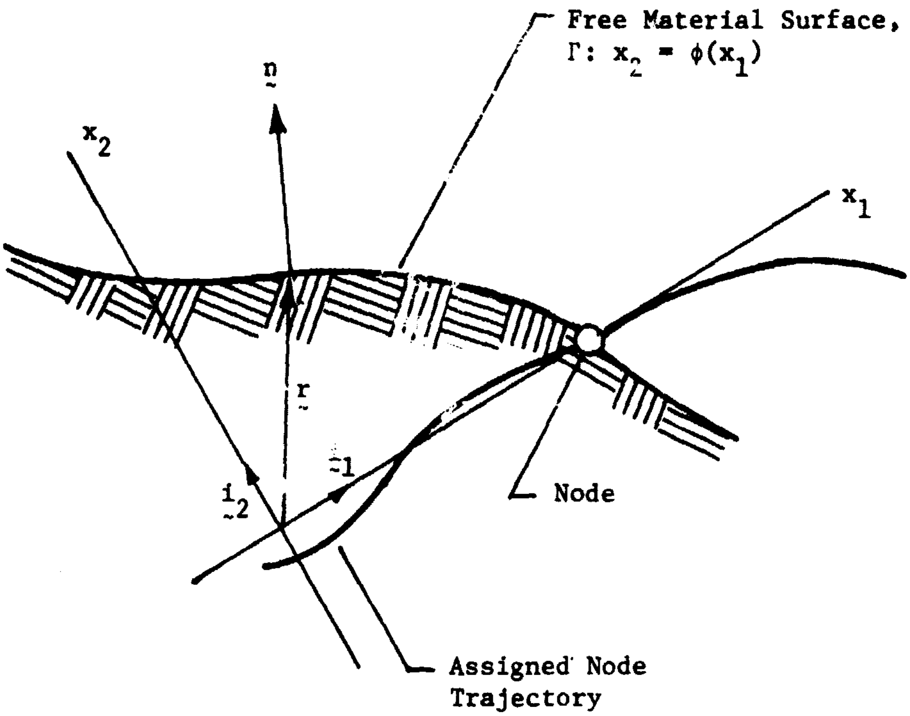

Fig. 7-1 - Geometry of Free Surface

and

$$v_n^G = v_n = (v_1 \underset{\sim}{i}_1 + v_2 \underset{\sim}{i}_2) \cdot \underset{\sim}{n}$$

$$= v_1 \frac{\phi'}{(1 + \phi'^2)^{1/2}} - v_2 \frac{1}{(1 + \phi'^2)^{1/2}}$$

If x_1 denotes a coordinate tangent to the node trajectory path, then $v^G = 0$, and we have the condition

$$v_1^G = v_1 - v_2 \frac{d\psi}{dx_2} \tag{7.2}$$

In general (for three dimensions), if Γ is given by an equation of the form

$$x_1 = \psi (x_2, x_3)$$

the interface condition is

$$v_1^G = v_1 - v_2 \frac{\partial\psi}{\partial x_2} - v_3 \frac{\partial\psi}{\partial x_3} \tag{7.3}$$

If Γ is a fluid-solid interface, we have

$$v_n^G = v_n^{Fluid} = v_n^{Solid} \quad \text{on } \Gamma \tag{7.4}$$

at all nodes on Γ.

8. A LINEAR FSI-MODEL FOR NEARLY INCOMPRESSIBLE VISCOUS FLOWS

8.1 GENERAL

We would like to construct a formulation of the fluid-structure interaction problem which has the following features:

1. Is applicable to the problem of a viscous incompressible or slightly compressible fluid interacting with an elastic solid.
2. Is characterized by linear equations.

Unfortunately, linear FSI-models for compressible flow almost exclusively deal with the small-perturbation acoustic approximations of plane or spherical waves impinging on an elastic body and these problems are of secondary interest here. We shall therefore, consider a model which arises from a penalty treatment of the continuity equation for incompressible viscous fluids, thereby allowing for a non-zero "bulk viscosity" of the fluid.

8.2 GOVERNING EQUATIONS OF THE FLUID

For the general Stokesian fluid, the governing equations of motion are:

<u>Continuity:</u>

$$\frac{\partial \rho}{\partial t} + v_k \rho_k + \rho v_{k,k} = 0 \tag{8.1}$$

<u>Momentum:</u>

$$\rho \frac{\partial v_k}{\partial t} + \rho v_j v_{k,j} = \rho b_k + \sigma_{kj,j} \tag{8.2}$$

Constitutive:

$$\sigma_{k_j} = (-\pi + \lambda d_{rr})\,\delta_{kj} + 2\mu\, d_{k_j} \qquad (8.3)$$

where

ρ = the fluid density

v_k = Cartesian components of velocity

b_k = body force density

σ_{k_j} = components of the Cauchy stress tensor

π = the thermodynamic pressure

$d_{ij} = \frac{1}{2}(v_{i,j} + v_{j,i})$ = the deformation rate

λ, μ = deletational and shear viscosities.

The thermodynamic pressure π is given in terms of ρ and the absolute temperature θ, by the equation of state of the fluid. Since we are ignoring thermal effects here, we have

Equation of State:

$$\pi = \pi(\rho) \qquad (8.4)$$

For polytropic gas, for example,

$$\pi(\rho) = p_o \rho^{\gamma} \qquad (8.5)$$

where p_o = constant and γ is a material constant.

Upon substituting Eq. (8.3) into Eq. (8.2), we obtain the Navier-Stokes equations for isothermal, viscous, compressible flow:

$$\rho \frac{\partial v_k}{\partial t} + \rho v_j\, v_{k,j} = \rho b_k - \pi_k + (\lambda + \mu)\, v_{j,jk} + \mu v_{k,jj} \qquad (8.6)$$

which can also be written in the vector form

$$\rho \dot{\underset{\sim}{v}} = \underset{\sim}{b} - \underset{\sim}{\nabla}\pi + (\lambda + 2\mu)\underset{\sim}{\nabla} (\underset{\sim}{\nabla} . \underset{\sim}{v}) - \mu\underset{\sim}{\nabla} \times \underset{\sim}{\nabla} \times \underset{\sim}{v} \qquad (8.7)$$

where v is the material time derivative of the velocity:

$$\dot{\underset{\sim}{v}} = \frac{D\underset{\sim}{v}}{Dt} = \frac{\partial \underset{\sim}{v}}{\partial t} + \underset{\sim}{v} . \underset{\sim}{\nabla} \underset{\sim}{v} \qquad (8.8)$$

8.3 A PENALTY FORMULATION

Let $\underset{\sim}{P}$ denote the vector defined by

$$\rho \underset{\sim}{P} = \rho(\dot{\underset{\sim}{v}} - \underset{\sim}{b}) + \mu\underset{\sim}{\nabla} \times \text{curl } \underset{\sim}{v} \qquad (8.9)$$

Then the equations of motion can be written compactly as

$$\begin{aligned} \dot{\rho} &= - \text{div } v \\ \rho \underset{\sim}{P} &= k\underset{\sim}{\nabla} \text{ div } \underset{\sim}{v} - \nabla\pi \end{aligned} \qquad (8.10)$$

where $k = \lambda^2 + \mu$ is a "bulk" viscosity for the fluid. In the case of an incompressible fluid, these equations reduce to

$$\begin{aligned} \text{div } \underset{\sim}{v} &= 0 \\ \rho \underset{\sim}{P} &= \underset{\sim}{\nabla} - \pi \end{aligned} \qquad (8.11)$$

where π is now the unknown hydrostatic pressure.

A <u>penalty approximation</u> of the incompressibility condition (div v = 0) in Eq. (8.11) yields alternatively, the modified momentum equation

$$\rho \underset{\sim}{P} = -\varepsilon^{-1} \underset{\sim}{\nabla} \text{ div } \underset{\sim}{v}_{\varepsilon} + k\underset{\sim}{\nabla} \text{ div } \underset{\sim}{v}_{\varepsilon} \qquad (8.12)$$

where ε is a positive number and one hopes that

$$\left.\begin{array}{l} \operatorname{div} \underset{\sim}{v}_{\varepsilon} \to 0 \\ \pi_{\varepsilon} \to \pi \end{array}\right\} \text{ as } \varepsilon \to 0 \tag{8.13}$$

with

$$\pi\varepsilon = -\varepsilon^{-1} \operatorname{div} \underset{\sim}{v}\varepsilon \tag{8.14}$$

and the convergence in Eq. (8.13) is in $(H'(\Omega))^N$ for $\underset{\sim}{v}_{\varepsilon}$ and $L^2(\Omega)$ for π_{ε}.

It is clear that

1. The penalized momentum (Eq. (8.12)) corresponds to that of a compressible fluid with an equation of state given by Eq. (8.14).
2. If this compressible fluid is characterized as a baratropic (?) gas according to Eq. (8.5), then the continuity equation is of the form

$$\dot{\rho} = \varepsilon\ p_0\, \rho^{\gamma+1} \tag{8.15}$$

3. Over any domain $\Omega_0 \subset \Omega$ on which $\rho_{,k} = 0$ (ρ varies only with time) we have

$$\int_0^t \frac{d\rho}{\rho^{1+\gamma}} = \varepsilon\ p_o\ t \tag{8.16}$$

that is, the density in Ω_0 can be determined by a quadrature.

We shall employ the approximations (Eq. (8.12) and Eq. (8.16)) in subsequent discussions.

8.4 GOVERNING EQUATIONS OF THE SOLID

The motion of an elastic solid is governed by the classical equations,

$$(E_{ijk\ell}\ u_{k,\ell})_{,j} + \rho_s\, f_i = \rho_s\, \ddot{u}_i \tag{8.17}$$

where

$E_{ijk\ell}$ = the elastic constants of the material (Hooke's tensor) exhibit standard symmetries and ellipticity

u_k = the Cartesian components of the displacement vector

ρ_s = the mass density of the solid

f_i = the components of body force of the solid

8.5 BOUNDARY AND INTERFACE CONDITIONS

Consider the geometrical situations and notations indicated in Fig. 8-1. In this case, the FSI-Problem is governed by the following equations.

Fluid

$$\left.\begin{aligned} \rho\dot{\underset{\sim}{v}} + (\varepsilon^{-1} - k)\,\underset{\sim}{\nabla}\,\mathrm{div}\,\underset{\sim}{v} + \mu\underset{\sim}{\nabla} \times \mathrm{curl}\,\underset{\sim}{v} &= \rho\underset{\sim}{b} \text{ in } \Omega_F \\ \underset{\sim}{v} &= \hat{\underset{\sim}{v}} \quad \text{on } \Gamma_{F1} \\ \underset{\sim}{t}_F &= \underset{\sim}{s}^F \quad \text{on } \Gamma_{F2} \end{aligned}\right\} \tag{8.18}$$

Fluid-Solid Interface

$$\underset{\sim}{v} = \dot{\underset{\sim}{u}} \quad \text{on } \Gamma_I \tag{8.19}$$

Solid

$$\left.\begin{aligned} \underset{\sim}{\nabla} \cdot \underset{\approx}{E}\,\underset{\sim}{u} + \rho_s \underset{\sim}{f} &= \rho_s \ddot{\underset{\sim}{u}} \quad \text{on } \Omega_s \\ \underset{\sim}{u} &= \underset{\sim}{0} \quad \text{on } \Gamma_{s1} \\ \underset{\sim}{n} \cdot \underset{\sim}{E}\,\underset{\sim}{u} &= S_s \quad \text{on } \Gamma_{s2} \end{aligned}\right\} \tag{8.20}$$

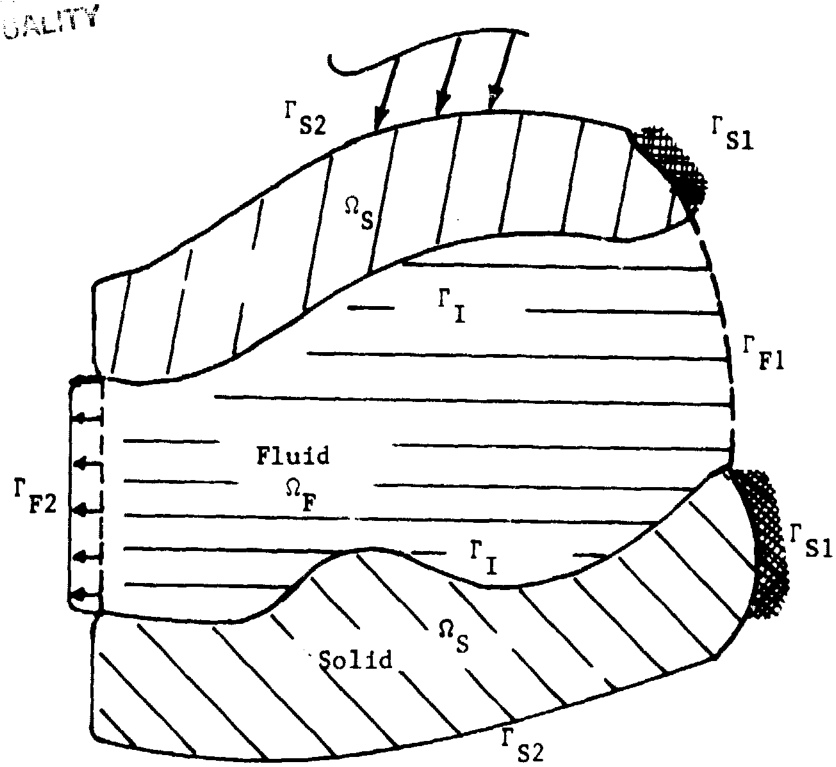

Fig. 8-1 - Fluid-Solid Interface

Initial Conditions

$$\left.\begin{aligned} \underset{\sim}{v}(\underset{\sim}{x},0) &= \underset{\sim}{v}_0 \quad \text{on } \Omega_F \\ \underset{\sim}{u}(\underset{\sim}{x},0) &= \underset{\sim}{u}_0 \quad \text{on } \Omega_s \\ \dot{\underset{\sim}{u}}(\underset{\sim}{x},0) &= \dot{u}_0 \quad \text{on } \Omega_s \\ v_0 &= u_0 \quad \text{on } \Gamma_1 \end{aligned}\right\} \tag{8.21}$$

In Eq. (8.18), $\underset{\sim}{v}$ and $\underset{\sim}{s}^F$ denote prescribed velocity or tractions along Γ_F, with

$$\underset{\sim}{s}^F = \underset{\sim}{n} \cdot \underset{\sim}{\sigma}^F(\underset{\sim}{v}) \tag{8.22}$$

where $\underset{\sim}{\sigma}^F(\underset{\sim}{v})$ is defined in Eq. (8.3) and $\underset{\sim}{n}$ is a unit vector exterior and normal to the surface Γ_F. The interface condition, Eq. (8.19) characterizes the so-called no-slip condition; i.e., the fluid is to adhere to the solid at the interface: to do otherwise would suggest a discontinuity in traction across the interface.

In certain instances which suggest that this no-slip condition be relaxed, we can use instead of Eq. (8.19) the slip-interface condition

$$\dot{u}_n = v_n; \quad (\dot{\underset{\sim}{u}} - \underset{\sim}{v}) \cdot \underset{\sim}{\tau} = \upsilon^F \cdot \tau \quad \text{on } \Gamma_I \tag{8.23}$$

where $u_n = \underset{\sim}{u} \cdot \underset{\sim}{n}$, $v_n = v \cdot \underset{\sim}{n}$, τ is a unit vector tangent to Γ_I, υ is a film coefficient (which may depend upon temperature and density of the fluid) and $\underset{\sim}{S}^F$ is given by Eq. (8.22).

8.6 VARIATIONAL FORMS

Let $\underset{\sim}{\psi} \epsilon \, (C^1(\overline{\Omega}_F))^3$ and $\varphi \epsilon \, (C^1(\overline{\Omega}_s))^3$ be sufficiently smooth vectors defined over $\overline{\Omega}_F$ and $\overline{\Omega}_s$, respectively. Taking the inner product of the momentum equations of the fluid and the solid with $\underset{\sim}{\psi}$ and $\underset{\sim}{\varphi}$, respectively, integrating over the respective domains, and applying the Green-Gauss theorem yields:

$$\left.\begin{aligned}
&\int_{\Omega_F} \rho v_k \psi_k \, dx + \int_{\Omega_F} [\mu v_{k,i} \psi_{k,i} + k_\epsilon \operatorname{div} \underset{\sim}{v} \operatorname{div} \underset{\sim}{\psi}] \, dx \\
&\qquad = \int_{\partial\Omega_F} \sigma^F{}_{ik}(\underset{\sim}{v}) \, n_i \psi_k \, ds + \int_{\Omega_F} \rho \underset{\sim}{b} \cdot \underset{\sim}{\psi} \, dx \\
&\int_{\Omega_S} \rho_s \ddot{u}_k \; {}_k \, dx + \int_{\Omega_S} E_{ijk\ell} \, u_{k,} \quad {}_{i,j} \, dx \\
&\qquad = \int_{\Omega_S} \rho_s \, f \cdot \varphi \, dx + \int_{\partial\Omega_S} \sigma^s{}_{ik}(\underset{\sim}{u}) \, n_i \varphi_k \, ds
\end{aligned}\right\} \tag{8.24}$$

wherein

$$\left.\begin{aligned} k_\varepsilon &= \lambda + \mu - \varepsilon^{-1} \\ \sigma^F_{ki}(\underset{\sim}{v}) &= \mu v_{i,k} + k_\varepsilon \operatorname{div} \underset{\sim}{v}\, \delta_{ik} \\ \sigma^S_{ki}(\underset{\sim}{u}) &= E_{kirs} u_{r,s} \end{aligned}\right\} \qquad (8.25)$$

on $\partial\Omega_F$ we take

$$\psi_k = 0 \quad \text{on } \overline{\Gamma}_{F1} \cup \overline{\Gamma}_I; \; \sigma^F_{ki}(\underset{\sim}{v})\, n_k = S^F_i \quad \text{on } \Gamma_{F2}$$

Thus,

$$\int_{\partial\Omega_F} \sigma^F_{ki}(\underset{\sim}{v})\, n_k\, \psi_i\, ds = \int_{\Omega_{F2}} S^F_k\, \psi_k\, ds$$

Similarly, with $\varphi_k = 0$ on $\Gamma_{S1} \cup \Gamma_I$,

$$\int_{\partial\Omega_S} \sigma^S_{ki}(u)\, n_k \quad {}_i\, ds = \int_{\Omega_{S2}} S^F_k\, \varphi_k\, ds$$

Thus, we arrive at the variational boundary-initial-value problem of finding $\underset{\sim}{v}(t)$, $\underset{\sim}{u}(t)$, $t \in [0,T]$, such that

$$\left.\begin{aligned} & \rho \dot{v}_k\, \psi_k\, dx + \int_{\Omega_F} \sigma^F_{ik}(\underset{\sim}{v})\, \psi_{k,i}\, dx \\ & = \int_{\Omega_F} \rho b_k\, \psi_k\, dx + \int_{\Gamma_{F2}} S^F_k\, \psi_k\, ds \\ & \int_{\Omega_S} \rho_S\, \ddot{u}_k\, \varphi_k\, dx + \int_{\Omega_S} \sigma^S_{ik}(\underset{\sim}{u})\, \varphi_{k,i}\, dx \\ & = \int_{\Omega_S} \rho_S\, f_k\, \varphi_k\, dx + \int_{\Gamma_{S2}} S^S_k\, \varphi_k\, ds \end{aligned}\right\} \qquad (8.26)$$

for all sufficiently smooth functions $\underset{\sim}{\psi}$, $\underset{\sim}{\varphi}$ which vanish on $\overline{\Gamma}_{F1} \cup \overline{\Gamma}_I$ and $\overline{\Gamma}_{S1} \cup \overline{\Gamma}_I$, respectively.

8.7 FINITE ELEMENT MODELS

We partition $\overline{\Omega} = \overline{\Omega}_F \cup \overline{\Omega}_S$ into finite elements in the usual manner. The approximate velocities and displacements are of the form

$$v_k = \sum_J v_k^J \psi_J \qquad u_k = \sum_J u_k^J \varphi_J \tag{8.27}$$

where v^J, u^J denote values of v_k and u_k at a nodal point J in the respective fluid and solid meshes. Introducing these approximations into Eq.(8.25) yields the corresponding element equations of motion in terms of the nodal values. The final system of equations for the discrete model is of the form

$$\begin{bmatrix} \underset{\approx}{M}_{FF} & \underset{\approx}{M}_{FI} & \underset{\approx}{0} \\ \underset{\sim}{M}_{IF} & \underset{\sim}{M}_{II} & \underset{\sim}{M}_{IS} \\ \underset{\sim}{0} & \underset{\sim}{M}_{SI} & \underset{\sim}{M}_{SS} \end{bmatrix} \begin{bmatrix} \dot{\underset{\sim}{v}}_F \\ \ddot{\underset{\sim}{u}}_I \\ \ddot{\underset{\sim}{u}}_S \end{bmatrix} + \begin{bmatrix} \underset{\sim}{K}^f_{FF} & \underset{\sim}{K}^f_{FI} & \underset{\sim}{0} \\ \underset{\sim}{K}^f_{IF} & \underset{\sim}{K}^f_{II} & \underset{\sim}{0} \\ \underset{\sim}{0} & \underset{\sim}{0} & \underset{\sim}{0} \end{bmatrix} \begin{bmatrix} \underset{\sim}{v}_F \\ \dot{\underset{\sim}{u}}_I \\ \dot{\underset{\sim}{u}}_S \end{bmatrix}$$

$$+ \begin{bmatrix} \underset{\sim}{0} & \underset{\sim}{0} & \underset{\sim}{0} \\ \underset{\sim}{0} & \underset{\sim}{K}_{IS} & \underset{\sim}{K}_{SS} \\ \underset{\sim}{0} & \underset{\sim}{K}_{SI} & \underset{\sim}{K}_{SS} \end{bmatrix} \begin{bmatrix} \underset{\sim}{v}_F \\ \underset{\sim}{u}_I \\ \underset{\sim}{u}_S \end{bmatrix} = \begin{bmatrix} \underset{\sim}{b} \\ \underset{\sim}{f}_I \\ \underset{\sim}{f} \end{bmatrix} \tag{8.28}$$

Here the matrices $\underset{\sim}{M}_{FF}$, ... , $\underset{\sim}{M}_{SS}$ are mass matrices, $\underset{\sim}{K}_{FF}$, ... are fluid "stiffness" matrices, $\underset{\sim}{K}_{IS}$,..., $\underset{\sim}{K}_{SS}$ are stiffness matrices for the solid. The vectors $\underset{\sim}{v}$ and $\underset{\sim}{u}$ of nodal values of velocity and displacement are partitioned into column vectors corresponding to nodes on the interior of the fluid/solid mesh and nodes on the fluid-structure interface:

$$v = \begin{bmatrix} v_F \\ v_I \end{bmatrix}, \quad u = \begin{bmatrix} u_I \\ u_S \end{bmatrix}$$

The no-slip interface condition enters the formulation by setting $\underset{\sim}{v}_I = u_I$. Hence, the division of nodal-point degrees of freedom in Eq. (8.28) corresponds to a convention of the type indicated in Fig. 8-2.

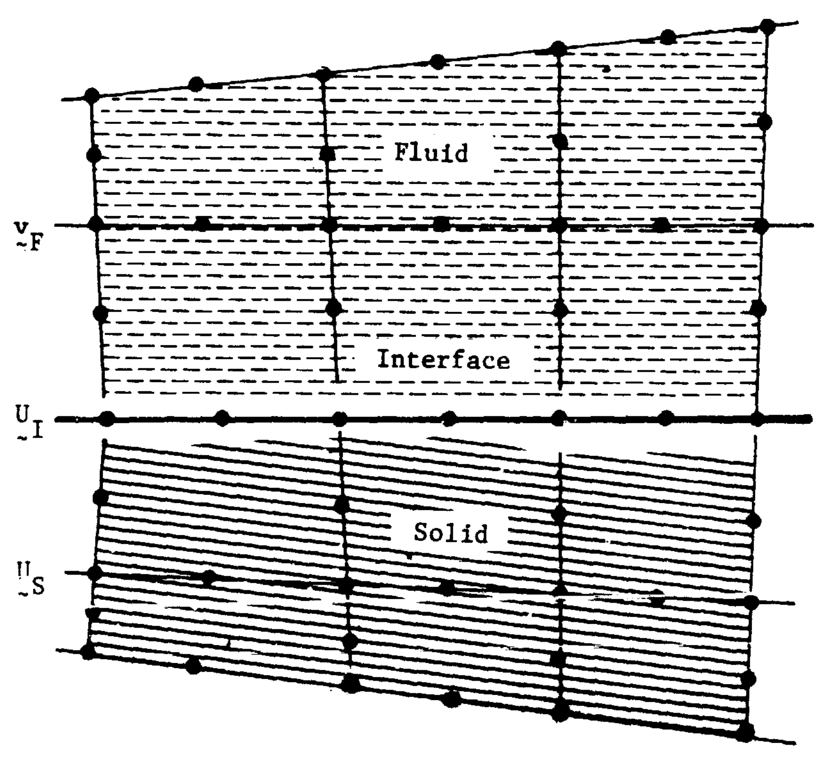

Fig. 8-2 - No-Slip Interface

Since $\underset{\sim}{M}_{FF}^{F}$ is invertible, the second equation (the interface equations) in Eq. (8.28) can be written

$$\bar{\underset{\sim}{M}}_{II}\,\ddot{\underset{\sim}{u}}_I + \underset{\sim}{M}_{IS}\,\ddot{\underset{\sim}{u}}_s + \bar{K}_{IF}^{f}\,v_F + \bar{\underset{\sim}{K}}_{II}^{f}\,\dot{\underset{\sim}{u}}_I + \underset{\sim}{K}_{II}\,\underset{\sim}{u}_I + \underset{\sim}{K}_{SS}\,\underset{\sim}{u}_S = \bar{\underset{\sim}{f}}_I \qquad (8.29)$$

where

$$\left.\begin{aligned}
\bar{\underset{\sim}{M}}_{II} &= \underset{\sim}{M}_{II} - \underset{\sim}{M}_{IF}\,\underset{\sim}{M}_{FF}^{-1}\,\underset{\sim}{M}_{FI}\\
\bar{K}_{IF}^{f} &= \underset{\sim}{K}_{IF}^{f} - \underset{\sim}{M}_{IF}\,\underset{\sim}{M}_{FF}^{-1}\,\underset{\sim}{K}_{FF}^{f}\\
\bar{K}_{II}^{f} &= \underset{\sim}{K}_{II}^{f} - \underset{\sim}{M}_{IF}\,\underset{\sim}{M}_{FF}^{-1}\,\underset{\sim}{K}_{FI}^{f}\\
\bar{\underset{\sim}{f}}_{I} &= \underset{\sim}{f}_{I} - \underset{\sim}{M}_{IF}\,\underset{\sim}{M}_{FF}^{-1}\,\underset{\sim}{b}
\end{aligned}\right\} \qquad (8.30)$$

(matrix condensation).

9. SPAR MODIFICATIONS FOR INCOMPRESSIBLE VISCOUS FLOW CALCULATIONS

9.1 ORIENTATION

In the standard program, SPAR computes the stiffness matrix $\underset{\sim}{k}$ for the four-node (E41) element by the formula

$$\underset{\sim}{k} = \underset{\sim}{T}^T \underset{\sim}{H}^{-1} \underset{\sim}{T}$$

where T and H are the matrices

$$\underset{\sim}{T} = \int_\Gamma \underset{\sim}{R}^T \underset{\sim}{L} \, ds, \quad \text{and}$$

$$\underset{\sim}{H} = \int_\Omega \underset{\sim}{P}^T \underset{\sim}{N} \underset{\sim}{P} \, dx \, dy.$$

In these formulas, the following notation is used:

- $\underset{\sim}{P}$ is the matrix defining the stress components $\underset{\sim}{\sigma} = \{\sigma_{11}, \sigma_{22}, \sigma_{12}\}^T$ in terms of the vector $\underset{\sim}{\beta}$ of stress degrees-of-freedom

$$\underset{\sim}{\sigma} = \underset{\sim}{P} \underset{\sim}{\beta} \quad (\text{Order } \underset{\sim}{P} = 3 \times 5)$$

- $\underset{\sim}{N}$ is the 3 x 3 matrix of material constants, and in the case of a viscous incompressible fluid is

$$\underset{\sim}{N} = \frac{1}{2\mu} \begin{bmatrix} 1 & 0 & 0 \\ 0 & 1 & 0 \\ 0 & 0 & 1 \end{bmatrix}$$

- Ω is the area of the element and Γ is its boundary

- $\underset{\sim}{R}$ is the matrix defining the surface tractions $\underset{\sim}{S} = \{S_1, S_2\}^T$ in terms of the stress parameters $\underset{\sim}{\beta}$:

$$\underset{\sim}{S} = \underset{\sim}{R} \underset{\sim}{\beta} \quad (\text{Order } \underset{\sim}{R} = 2 \times 5)$$

This corresponds to the Cauchy stress principle,

$$S_i = \sigma_{ij} n_j \implies \underset{2\times 1}{\underset{\sim}{S}} = \underbrace{\begin{bmatrix} n_1 & n_2 & 0 \\ 0 & n_1 & n_2 \end{bmatrix}}_{\hat{n}} \underset{3\times 1}{\underset{\sim}{\sigma}}$$

$$\underset{\sim}{S} = \underset{\sim}{\hat{n}}\,\underset{\sim}{\sigma} = \underset{\sim}{\hat{n}}\,\underset{\sim}{P}\,\underset{\sim}{\beta} = \underset{\sim}{R}\,\beta; \text{ i.e.,}$$

$$\boxed{\underset{\sim}{R} = \underset{\sim}{\hat{n}}\,\underset{\sim}{P} \qquad \underset{\sim}{\hat{n}} = \text{matrix of components of unit normal to } \Gamma}$$

- $\underset{\sim}{L}$ is the matrix defining the boundary displacements $\underset{\sim}{v} = \{v_1(s),\ v_2(s)\}^T$ in terms of the 8 x 1 vector $\underset{\sim}{q}$ of nodal displacement degrees of freedom

$$\underset{\sim}{v} = \underset{\sim}{L}\,\underset{\sim}{q} \qquad (\text{Order } \underset{\sim}{L} = 2 \times 8)$$

9.2 Q MATRIX CALCULATION

We wish to compute an additional matrix $\underset{\sim}{Q}$ that is similar to $\underset{\sim}{T}$ except that it is of order 1 x 8:

$$\underset{1\times 8}{\underset{\sim}{Q}} = \int_{\Omega} \underset{1\times 2}{[n_1,\ n_2]}\ \underset{2\times 8}{\underset{\sim}{L}}\ ds$$

The computation of $\underset{\sim}{Q}$ proceeds as follows:

Using the notation below

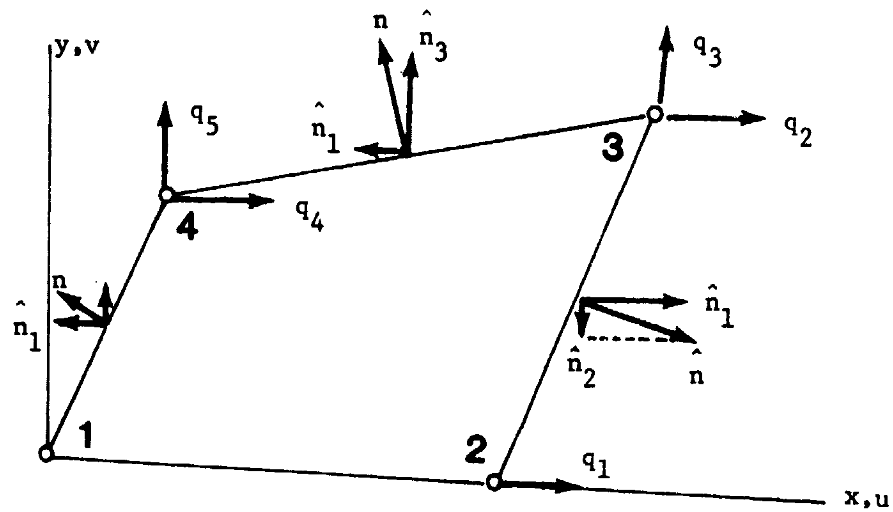

Along boundary 1-2

$$\int_1^2 = \int_0^{x_2} (\hat{n}_1 u + \hat{n}_1 v)\, ds$$

$$\hat{n}_1 = 0, \quad \hat{n}_2 = -1$$

$$u = q_1, \quad v = 0, \quad ds = dx$$

$$\int_1^2 = \int_0^{x_2} [(0)\, q_1 + (-1)\,(0)]\, dx = 0$$

Along boundary 2-3

$$\int_2^3 = \int_0^{y_3} (\hat{n}_1 u + \hat{n}_2 v)\, ds$$

where

$$\ell = \sqrt{(x_3 - x_2)^2 + y_3^2}$$

$$\hat{n}_1 = \frac{y_3}{\ell}, \quad \hat{n}_2 = \frac{x_2 - x_3}{\ell}, \quad ds = \frac{\ell}{y_3}\, dy$$

$$u = (1 - \frac{y}{y_3})\, q_1 + \frac{y}{y_3}\, q_2, \quad u = \frac{y}{y_3}\, q_3$$

$$\int_2^3 = \int_0^{y_3} \left[(1 - \frac{y}{y_3})\, q_1 + \frac{y}{y_3}\, q_2 + (x_2 - x_3)\, \frac{y}{y_3^2}\, q_3\right] dy$$

$$= \frac{y_3}{2}\, q_1 + \frac{y_3}{2}\, q_2 + \frac{(x_2 - x_3)}{2}\, q_3$$

Along boundary 3-4 .

$$\int_3^4 = \int_{x_3}^{x_4} (\hat{n}_1\, u + \hat{n}_2\, v)\, ds$$

where

$$\ell = \sqrt{(x_3 - x_4)^2 + (y_3 - y_2)^2}$$

$$n_1 = \frac{y_4 - y_3}{\ell}, \quad \hat{n}_2 = \frac{x_3 - x_4}{\ell}$$

$$u = \left[1 - \left(\frac{x - x_4}{x_3 - x_4}\right)\right] q_4 + \left(\frac{x - x_4}{x_3 - x_4}\right) q_2$$

$$v = \left[1 - \left(\frac{x - x_4}{x_3 - x_4}\right)\right] q_5 + \left(\frac{x - x_4}{x_3 - x_4}\right) q_3$$

$$ds = \left(\frac{\ell}{x_4 - x_3}\right) dx$$

$$\int_3^4 = \int_{x_3}^{x_4} \left\{\left[\frac{y_4 - y_3}{\ell}\right] \left[\left(1 - \left(\frac{x - x_4}{x_3 - x_4}\right)\right) q_4 + \left(\frac{x - x_4}{x_3 - x_4}\right) q_2\right]\right.$$

$$\left. + \left[\frac{x_3 - x_4}{\ell}\right] \left[\left(1 - \left(\frac{x - x_4}{x_3 - x_4}\right)\right) q_5 + \left(\frac{x - x_4}{x_3 - x_4}\right) q_3\right]\right\} \frac{\ell\, dx}{(x_4 - x_3)}$$

$$= \frac{(y_4 - y_3)}{2} q_4 + \frac{(y_4 - y_3)}{2} q_2 - \frac{(x_4 - x_3)}{2} q_5 - \frac{(x_4 - x_3)}{2} q_3$$

Along boundary 4-1

$$\int_4^1 = \int_{y_4}^{y_1} (\hat{n}_1 u + \hat{n}_2 v)\, ds$$

where

$$\ell = \sqrt{x_4^2 - y_4^2}$$

$$\hat{n}_1 = \frac{y_4}{\ell}, \qquad \hat{n}_2 = \frac{x_4}{\ell}$$

$$u = \frac{y}{y_4} q_4, \qquad v = \frac{y}{y_4} q_5, \qquad ds = -\frac{\ell}{y_4} dy$$

$$\int_4^1 = - \int_{y_4}^{0} \left(- y\, q_4 + \frac{x_4}{y_4}\, y\, q_5\right) \frac{dy}{y_4}$$

$$= \frac{x_4}{2}\, q_5 - \frac{y_4}{2}\, q_4$$

$$\int_{\Gamma} = \int_1^2 + \int_2^3 + \int_3^4 + \int_4^1$$

$$Q = \frac{1}{2}\left[y_3 q_1 + y_4 q_2 + (x_2 - x_4)\, q_3 - y_3 q_4 + x_3 q_5\right]$$

9.3 THE NEW PENALIZED STIFFNESS MATRIX

We are now ready to compute the new stiffness matrix for the incompressible viscous flow problem.

Step 1: Compute the usual stiffness matrix K^o using $N = \frac{1}{2\mu} \underset{\sim}{I}_{3x3}$

$$\underset{\sim}{K}^o = \underset{\sim}{T}^T \underset{\sim}{H}^{-1} \underset{\sim}{T}$$

Step 2: Let A_e denote the area of the element. Using the Q matrix discussed earlier, compute the perturbation stiffness matrix

$$\underset{\sim}{K}_{\varepsilon} = -\frac{1}{\varepsilon} \cdot \frac{1}{A_e} \underset{\sim}{Q}^T \underset{\sim}{Q}$$

Step 3: Add $\underset{\sim}{K}$ and $\underset{\sim}{K}_{\varepsilon}$ to get the element stiffness matrix

$$\underset{\sim}{K} = \underset{\sim}{K}^o + \underset{\sim}{K}_{\varepsilon}$$

The theory behind these calculations is given in Appendix A.

These modifications have been incorporated into the SPAR code. Update pages to the SPAR user's guide are presented in Appendix B.

10. RESULTS

Solutions were attempted for four two-dimensional example problems. The first three consisted of viscous flow of an incompressible fluid within rigid boundaries. The fourth problem consisted of two elastic plates coupled by a Stokesian fluid. Reasonable results were obtained for the velocity field for the first three problems. Descriptions of the example problems with sketches, finite element grids, SPAR input data listings, and tabulated results, are presented in Appendixes C through E. A pressure calculation routine was implemented but calculated pressures were not reasonable and no results are presented in this report.

The first example (Appendix C) consists of parallel flow through a straight channel with uniform pressure boundary conditions applied at the entrance and exit of the channel. This problem has a linear pressure distribution in the flow direction and a parabolic velocity profile in the transverse direction. An 8 x 8 element mesh was used. A plot of the finite element grid, with the transverse scale enlarged for clarity, is shown. As can be seen from the tabulated results, the velocity remained essentially constant in the flow direction verifying that incompressibility is enforced.

The second example (Appendix D) is a plane slider bearing lubrication problem. This problem consists of a moving guide surface separated from a stationary slide block by an incompressible viscous lubricant. As can be seen from the dimensions on the sketch, this model has a length-to-width ratio of 900. This caused a problem with element aspect ratios in SPAR with an 8 x 8 mesh, so an 8 x 18 mesh was used for this problem. Again, a plot of the model with the y-direction scale enlarged for clarity is shown. The computed velocities agreed very well with the analytical values.

The third example (Appendix E) consists of incompressible flow in a driven cavity. The problem consists of a square box enclosed on three sides containing a viscous incompressible fluid driven on the upper surface with a uniform velocity.

REFERENCES

1. Belytschko, T., "Methods and Programs for Analysis of Fluid-Structure Systems," Nuclear Engineering and Design, Vol. 42, 1977, pp. 41-52.

2. Belytschko, T., "Fluid-Structure Interaction," Computers and Structures, Vol. 12, 1980, pp. 459-469.

3. Kennedy, J., and T. Belytschko, "Theory and Application of a Quasi-Eulerian Fluid Element for the Straw Code," ANL-78-100, October 1978.

4. Kennedy, J.M., Belytschko, T.B., H.S. Lee, and D.F. Schoeberle, "Coupled Fluid-Above-Core Structure Analysis," ANL/RAS 81-5, February 1981.

5. Kennedy, J.M. and T.B. Belytschko, "A Survey of Computational Methods for Fluid Structure Analysis of Reactor Safety," Document prepared by Reactor Analysis and Safety Division, Argonne National Laboratory.

6. Belytschko, T.B. and Kennedy, J.M., "Computer Models for Subassemble Simulation," Nuclear Engineering and Design, Vol. 49, 1978, pp. 17-38.

7. Belytschko, T.B. and J.M. Kennedy, "A Fluid-Structure Finite Element Method for the Analysis of Reactor Safety Problems," Nuclear Engineering and Design, Vol. 38, 1976, pp. 78-81.

8. Donea, J., P. Fasoli-Stella, and S. Giuliani, "Lagrangian and Eulerian Finite Element Techniques for Transient Fluid-Structure Interaction Problems," Trans. 4th International Copnf. of Struct. Mech. in Reactor Tech. San Francisco, 15-19 August 1977.

9. Donea, J., S. Guiliani, H. Laval, and H. Quaztapelle, "Finite Element Solution of the Unsteady Navier-Stokes Equations by a Fractional Step Method," Computer Methods in Appl. Mech. and Eng., Vol. 30, 1982, pp. 53-73.

10. Donea, J., P. Fasoli Stella, S. Giuliani, J.P. Halleux, and A.V. Jones, "Arbitrary Lagrangian Eulerian Finite Element Procedure for Transient Dynamic Fluid-Structure Interaction Problems," Comm. of the Eur. Communities, Isroa, Italy, 13-17 August 1979, North-Holland Publ. Co., Amsterdam.

11. Donea, J., S. Giuliani, and J.P. Halleux, "An Arbitrary Lagrangian-Eulerian Finite Element Method for Transient Dynamiac Fluid-Structure Interactions," Computer Methods in App. Mech. and Eng., Vol. 33, 1982, pp. 689-723.

12. Donea, J., "Finite Element Analysis of Transient Dynamic Fluid-Structure Interaction," Advanced Structural Dynamics, Edited by J. Donea, Applied Science Publishers Ltd., Essex, U.K., 1980, pp. 255-290.

13. Liu, W.K., "Development of Finite Element Procedures for Fluid-Structure Interaction," Ph.D. Dissertation, California Institute of Technology, Pasadena, 1980.

14. Kennedy, J., T. Belystchko, and D. Schoeberle, "A Quasi-Eulerian Fluid-Structure Code for Simulation of High-Pressure Transients in Core Components," Nuclear Technology, Vol. 51, 1980.

15. Chang, Y.W. and C.Y. Wang, "An Eulerian Method for Large Fluid-Structure Interaction in Reactor Components," Computational Methods for Fluid-Structure Interaction Problems, AMD-Vol. 26, ASME, 1977, pp. 1-14.

16. Harlow, F.R. and A.A. Amsden, "A Numerical Fluid Dynamics Calculation Method for all Flow Speeds," J. Comp. Physics, Vol. 8, 1971, pp. 197-213.

17. Wang, C.Y., "ICECO - An Implicit Eulerian Method for Calculating Fluid Transients in Fast-Reactor Containment," ARL-75-81, Argonne National Laboratory, Argonne, 1975.

18. Dianes, J.K., C.W. Hirt, and L.R. Stein, "Multi-Dimensional Fluid-Structure Interactions in a Pressurized Water Reactor," Computational Methods for Fluid-Structure Interaction Problems, AMD-Vol. 26, ASME, 1977, pp. 15-34.

19. Truesdell, C.A., "The Mechanical Foundations of Elasticity and Fluid Mechanics," J. Rotaional Mech. Anal., Vol. 1, pp. 125-300, Vol. 3, pp. 393-616, 1952.

20. Frank and Lazarus, "Mixed Eulerian-Lagrangian Methods," Methods in Computational Physics, Vol. 3, (B. Adler, ed.), Academic Press, New York, 1964.

21. Noh, W.F., "CEL - A Time-Dependent, Two-Space Dimensional, Coupled Eulerian-Lagrangian Code," Methods in Computational Physics, Edited by B. Alder et al., Academic Press, N.Y., 1964, p. 17.

22. Trulio, J.G., "Theory and Structure of AFTON Codes," Air Force Weapons Laboratory, Kirkland Air Force Base Report No. AFWL-TR-19, 1966.

23. Amsden, A.A. and C.W. Hirt, "YAQUI-An Arbitrary Lagrangian-Eulerian Computer Program for Fluid Flow at all Speeds," Report LA-5100, Los Alamos Scientific Laboratory, Los Alamos, N.M., March 1973.

24. Belytschko, T., J.M. Kennedy, and D.F. Schoeberle, "Quasi-Eulerian Finite Element Formulation for Fluid-Structure Interaction," J. Pressure Vessel Tech., Vol. 102, 1980, pp. 62-69.

25. Hughes, T.J.R., W.K. Liu, and T.K. Zimmermann, "Lagrangian-Eulerian Finite Element Formulation for Incompressible Viscous Flows," Computer Methods in Appl. Mech. and Eng., Vol. 29, 1981, pp. 329-349.

26. Liu, W.K., and D.C. Ma, "Computer Implementation Aspects for Fluid-Structure Interaction Problems," Computer Methods in Appl. Mech. and Eng., Vol. 31, 1982, pp. 129-148.

27. Belytschko, T., D.P. Flanagan, and J.M. Kennedy, "Finite Element Methods with User-Controlled Meshes for Fluid-Structure Interaction," Computer Meth. in Appl. Mech. and Eng., Vol. 33, 1982, pp. 669-688.

BIBLIOGRAPHY

Bathe, K.J. and V. Sonnad, "On Effective Implicit Time Integration in Analysis of Fluid-Structure Problems," Intl. J. for Num. Methods in Eng., 1980.

Belytschko, T.B., "Methods and Programs for Analysis of Fluid-Structure Systems," Nuclear Engineering and Design, Vol. 42, 1977, pp. 41-52.

Belytschko, T.B. and J.M. Kennedy, "Computer Models for Subassemble Simulation," Nuclear Engineering and Design, Vol. 49, 1978, pp. 17-38.

Belytschko, T.B. and J.M. Kennedy, "A Fluid-Structure Finite Element Method for the Analysis of Reactor Safety Problems," Nuclear Engineering and Design, Vol. 38, 1976, pp. 78-81.

Belytschko, T.B., J.M. Kennedy, and D.F. Schoeberle, "Quasi-Eulerian Finite Element Formulation for Fluid-Structure Interaction," J. of Pres. Vessel Tech., Vol. 102, 1980, pp. 62-69.

Belytschko, T., D.P. Flannagan, and J.M. Kennedy, "Finite Element Methods with User-Controlled Meshes for Fluid-Structure Interaction," Computer Meth. in Appl. Mech. and Eng., Vol. 33, 1982, pp. 669-688.

Belytschko, T.B., "Fluid-Structure Interaction," Computers and Structures, Vol. 12, 1980, pp. 459-469.

Belytschko, T.B., and R. Mullen, "Two-dimensional Fluid-Structure Impact Computations with Regularization," Computer Methods in Appl. Mech. and Eng., Vol. 27, 1981, pp. 139-154.

Belytschko, T.B., H.J. Yen, and R. Mullen, "Mixed Methods for Time Integration," Computer Methods in Appl. Mech. and Eng., Vol. 17/18, 1979, pp. 259-275.

Boris, J.P., and D.L. Book, "Flux-Corrected Transport. I. SHASTA, a Fluid Transport Algorithm that Works," J. Comp. Phys., Vol. 11, 1973, pp. 38-69.

Brown, S.J. and K.H. Hsu, "Use of the Finite Element Displacement Method to Solve Solid-Fluid Interaction Vibration Problems," Proceedings of the ASME Meeting, San Francisco, 1978.

Chang, Y.W., H.Y. Chu, J. Guildys, and C.Y. Wang, "Evaluation of Lagrangian, Eulerian, Arbitrary Lagrangian-Eulerian Methods for the Fluid-Structure Interaction Problems in ACDA Analysis."

Donea, J., "Finite Element Analysis of Transient Dynamic Fluid-Structure Interaction," Adv. Struct. Dynamics, Edited by J. Donea, Applied Science Publishers Ltd., Essex, U.K., 1980, pp. 255-290.

Donea, J., P. Fasoli-Stella, and S. Giuliani, "Lagrangian and Eulerian Finite Element Techniques for Transient Fluid-Structure Interaction Problems," Tran. 4th Intl. Conf. of Struct. Mech. in Reactor Technology, San Francisco, 15-19 August 1977.

Donea, J., P. Fasoli Stella, S. Giuliani, J.P. Halleux, and A.V. Jones, "Arbitrary Lagrangian Eulerian Finite Element Procedure for Transient Dynamic Fluid-Structure Interaction Problems," Comm. of the Eur. Communities, Isroa, Italy, 13-17 August 1979, North-Holland Publ. Co., Amsterdam.

Donea, J., P. Fasoli-Stella, S. Giuliani, J.P. Halleux, and A.V. Jones, Computer Code EURDYN - 1 M for Transient Dynamic Fluid-Structure Interaction. Pt. 1: Governing Equations and Finite Element Modeling, 1980.

Donea, J., S. Guiliani, H. Laval, and H. Quaztapelle, "Finite Element Solution of the Unsteady Navier-Stokes Equations by a Fractional Step Method," Computer Meth. in Appl. Mech. and Eng., Vol. 30, 1982, pp. 53-73, 1982.

Donea, J., S. Giuliani, and J.P. Halleux, "An Arbitrary Lagrangian-Eulerian Finite Element Method for Transient Dynamic Fluid-Structure Interactions," Computer Meth. in Appl. Mech. and Eng., Vol. 33, 1982, pp. 689-723.

Everstine, G.C., "Symmetric Potential Formulation for Fluid-Structure Interaction," J. Sound Vibration, Vol. 79, No. 1, Nov. 8, 1981, pp. 157-160.

Felippa, C.A., "A Family of Early-Time Approximations for Fluid-Structure Interaction," J. Appl. Mech., Vol. 47, 1980, pp. 703-708.

Felippa, C.A., "Top-Down Derivation of Doubly Asymptotic Approximations for Structure - Fluid Interaction Analysis," Proc. Second Int. Symp. on Innovative Numerical Analysis for the Enana. Sci., Montreal, Canada, 1980.

Felippa, C.A., and K.C. Park, "Staggered Transient Analysis Procedures for Coupled Mechanical Systems: Formulations," Computer Meth. in Appl. Mech. and Eng., Vol. 24, 1980, pp. 61-111.

Frank and Lazarus, "Mixed Eulerian-Lagrangian Methods," Methods in Computational Physics, Vol. 3, (B. Adler, ed.), Academic Press, New York, 1964.

Geers, T.L., "Doubly Asymptotic Approximations for Transient Motions of Submerged Structures," J. Acous. Soc. Am., Vol. 64, No. 5, 1978, pp. 1500-1508.

Geers, T.L., W.A. Loden, and H.C. Yee, "Boundary Element Analysis of Fluid-Solid Impact," Computational Methods for Fluid-Structure Interaction Problems, (T. Belytschko and T.L. Geers, eds.), Appl. Mech. Symposia Series, ASME, New York, 1977.

Geers, T.L., "Residual Potential and Approximate Methods for Three-Dimensional Fluid-Structure Interaction Problems," J. Acous. Soc. Am., Vol. 49, No. 5-2, 1981.

Giencke, E., and M. Forkel, "Difference Analysis for Fluid-Structure Interaction," Trans. Int. Conf. Struct. Mech. React. Tech. 5th, Vol. V, North-Holland Publishing Co., 1979.

Hamdi, M.A., Y. Ouseet, and G. Verchery, "A Displacement Method for the Analysis of Vibrations of Coupled Fluid-Structure Systems," Intl. J. Num. Meth. Eng., Vol. 13, 1978, pp. 139-150.

Harlow, F.H., and A.A. Amsden, "A Numerical Fluid Dynamics Calculation Method for all Flow Speeds," J. Comp. Phys., Vol. 8, 1971, pp. 197-213.

Haywood, J.H., "Response of an Elastic Cylindrical Shell to a Pressure Pulse," Quart. J. Mech. and Appl. Math., Vol. XI-2, 1958.

Heinrich, J., P. Huyakorn, O.C. Zienkiewicz, and A. Mitchell, "An 'Upwind' Finite Element Scheme for Two-Dimensional Convective Transport Equation," Intl. J. Num. Meth. in Eng., Vol. 11, 1977, pp. 131-143.

Hirt, C.W., A.A. Amsden, and J.L. Cook, "An Arbitrary Lagrangian-Eulerian Computing Method for all Flow Speeds," J. Comp. Phys., Vol. 14, 1974, pp. 227-253.

Hirt, C.W., J.L. Cook, and T.D. Butler, "A Lagrangian Method for Calculating the Dynamics of an Incompressible Fluid with Free Surface," J. Comp. Phys., Vol. 5, 1970, pp. 103-124.

Huang, H., "Transient Response of Two Fluid-Coupled Cylindrical Elastic Shells to an Incident Pressure Pulse," J. Appl. Mech., Vol. 46, 1979, pp. 513-518.

Huang, H., Everstine, G.C., and Y.F. Wang, "Retarded Potential Techniques for the Analysis of Submerged Structures Impinged by Weak Shock Waves," Comp. Meth. for Fluid-Struc. Interaction Problems, (T. Belytschko and T.L. Geers, eds.) Appl. Mech. Symposia Series, ASME, New York, 1977.

Hughes, T.J.R., "New Concepts in Finte Element Analysis," Applied Mechanics Conference, 1981.

Hughes, T.J.R., "Recent Developments in Computer Methods for Structural Analysis," Nucl. Eng. Des., Vol. 57, No. 2, 1980.

Hughes, T. and W. Liu, "Implicit-Explicit Finite Elements in Transient Analysis: Stability Theory," J. Appl. Mech., Vol. 45, 1978, pp. 371-374.

Hughes, T. and W. Liu, "Implicit-Explicit Finite Elements in Transient Analysis: Implementation and Numerical Examples," J. Appl. Mech., Vol. 45, 1978, pp. 375-378.

Hughes, T.J.R., Wina Kam Liu, and Thomas K. Zimmermann, "Lagrangian-Eulerian Finite Element Formulation for Incompressible Viscous Flows," CMAME, Vol. 29, No. 3, 1981, pp. 329-349.

Hughes, T.J.R., W.K. Liu, and T.K. Zimmermann, "Lagrangian-Eulerian Finite Element Formulation for Incompressible Viscous Flows," Computer Methods in Appl. Mech. and Eng., Vol. 29, 1981, pp. 329-349.

Kennedy, J., T. Belystchko, and D. Schoeberle, "A Quasi-Eulerian Fluid-Structure Code for Simulation of High-Pressure Transients in Core Components," Nuclear Technology, Vol. 51, 1980.

Kennedy, J., and T.B. Belytschko, "Theory and Application of a Quasi-Eulerian Fluid Element for the Straw Code," ANL-78-100, October 1978.

Kennedy, J.M., and T.B. Belytschko, "Theory and Application of a Finite Element Methods for Arbitrary Lagrangian-Eulerian Fluids and Structures," Nuclear Engineering and Design, Vol. 68, 1981, pp. 129-146.

Kennedy, J.M., T.B. Belytschko, H.S. Lee, and D.F. Schoeberle, "Coupled Fluid-Above-Core Structure Analysis," ANL/RAS 81-5, February 1981.

Kennedy, J.M., and T.B. Belytschko, "A Survey of Computational Methods for Fluid Structure Analysis of Reactor Safety," Document prepared by Reactor Analysis and Safety Division, Argonne National Laboratory.

Kot, C.A., B.J. Hsien, C.K. Youngdahl, and R.A. Valentin, "Transient Cavitation Phenomena in Fluid-Structure Interactions," Proc. Third Int. Conf. on Pressure Surges, Vol. 1, BARA Fluid Enana, 1980.

Kulak, R.F., "Finite Element Formulation for Fluid-Structure Interaction in Three-Dimensional Space," J. Pres. Vessel Tech. Trans. ASME, Vol. 103, No. 2, 1981, pp. 183-190.

Kulak, R.F., "Three-Dimensional Finite Element Formulation for Fluid-Structure Interaction," Trans. Int. Conf. Struct. Mech. React. Technol. 5th, Vol. B, 1979.

Kulak, R.F., "A Three-Dimensional Quasi-Eulerian Approach for Fluid-Structure Interaction Calculations," ASME, New York, 1980.

Kulak, R.F., "A Finite Element Formulation for Fluid-Structure Interaction in Three-Dimensional Space," Dynamics of Fluid-Structure Systems in the Energy Industry, Proc. 3rd Nat. Congress on Pressure Vessel and Piping, San Francisco, 25-29 June 1979.

Kulak, R.F., "Three-Dimensional Finite Element Formulation for Fluid-Structure Interaction," International Conference on Structural Mechanics in Reactor Technology, Berlin, Germany, 13 August 1979.

Liu, J.J., W.K. Liu, and A. Brooks, "Finite Element Anaysis of Incompressible Viscous Flows by the Penalty Function Formulation," J. Comp. Phys., Vol. 30, 1979, pp. 1-60.

Liu, W.K., "Development of Finite Element Procedures and Computer Implementation Aspects in Fluid-Structure Interactions," ASME, 1981, pp. 247-268.

Liu, W.K., and D.C. Ma, "Computer Implementation Aspects for Fluid-Structure Interaction Problems," Computer Methods in Appl. Mech. and Eng., Vol. 31, 1982, pp. 129-148.

Liu, W.K., "Development of Finite Element Procedures for Fluid-Structure Interaction," EERL 80-06, California Institute of Technology, Pasadena, 1981.

McMaster, W.H., E.Y. Gons, C.S. Landram, and D.F. Quinones, "Fluid Structure Coupling Algorithm," Symposium on Computational Methods in Nonlinear Structural and Solid Mechanics, Arlington, Va., 6 October 1980.

Morand, H., and R. Dhayon, "Substructure Variational Analysis of the Vibrations of Coupled Fluid/Structure Systems, Finite Element Results," Int. J. Numer. Methods in Engr., Vol. 14, No. 5, 1979, pp. 741-755.

Muller, M., "Simplified ANalysis of Linear Fluid-Structure Interaction," Intl. J. Num. Meth. in Eng., Vol. 17, 1981, pp. 113-121.

Nahavandi, A.N., "Finite Element Model for Fluid-Structure Interaction Studies," Trans. Int. Conf. Struct. Mech. React. Tech. 5th, Vol. B, Therm. and Fluid/Struct. Dyn. Anal., Berlin, Germany, Publ. by North-Holland Publ. Co., 1979.

Naganvandi, A.N., and R.R. Pedrido, "An Analysis of Solid-Fluid Interaction Using the Finite Element Method," Dynamic Analysis of Pressure Vessel and Piping Components, 18-23 September 1977.

Oesterle, B., and W. Ch. Mueller, "Finite Element Analysis of Fluid-Structure Interaction Problems," Trans. Int. Conf. Struct. Mech. React. Technol. 5th, Vol. B., Publ. by North-Holland Publ. Co., 1979.

Paidoussis, M.P., N.T. Issiol, and M. Tsui, "Parametric Resonance Oscillations of Flexible Slender Cylinders in Harmonically Perturbed Axial Flow. Part 1: Theory," J. Appl. Mech., Vol. 47, 1980, pp. 709-714.

Park, K.C., C.A. Felippa, and J.A. DeRuntz, "Stabilization of Staggered Solution Procedures for Fluid-Structure Interaction Analysis," Computational Methods for Fluid-Structure Interaction Problems, (T. Belytschko and L.T. Geers, eds.), Appl. Mech. Symposia Series, ASME, New York, 1977.

Sarpkaya, T., "Vortex-Induced Oscillations. A Selective Review," J. Appl. Mech., Vol. 46, 1979, pp. 241-258.

Tassoulas, J.L., E. Kausel, and M. Roesset, "Consistent Boundaries for Semi-Infinite Problems," Winter Annual Meeting of ASME, 15-20 November, 1981, Publ. ASME.

Wellford, L.C., and T.H. Ganaba, "A Finite Element Method with a Hybrid Lagrange Line for Fluid Mechanics Problems Involving Large Free Surface Motion," Intl. J. for Num. Meth. in Eng., Vol. 17, 1981, pp. 1201-1231.

Wilton, D., "Acoustic Radiation and Scattering From Elastic Structures," Intl. J. for Num. Meth. in Eng., Vol. 13, 1978, pp. 123-138.

Zienkiewicz, O.C., and P. Bettes, "Fluid-Structure Interaction and Wave Forces. An Introduction to Numerical Treatment," Intl. J. for Num. Meth. in Eng., Vol. 13, 1978, pp. 1-16.

Zienkiewicz, O.C., and P. Bettess, "Infinite Elements in the Study of Fluid-Structure Interaction Problems," Proc. Second Int. Symp. on Computing Methods in Applied Sciences, Rocquencourt, France, 15-19 December 1975.

Appendix A

A MODIFIED HELLINGER-REISSNER FORMULATION

Appendix A

The following equations govern the steady uniform flow of a viscous incompressible fluid:

$$\left.\begin{array}{l} \left.\begin{array}{l} \sigma'_{ij,j} - p_{,i} = f_i \\ d_{ij} \equiv \frac{1}{2} (v_{i,j} + v_{j,i}) \\ d_{ij} = \frac{1}{2\mu} \sigma'_{ij} \\ d_{kk} = \operatorname{div} \underset{\sim}{v} = 0 \end{array}\right\} \text{ in } \Omega \\ n_j (\sigma'_{ij} - p\, \delta_{ij}) = S_i \text{ on } \Gamma_\sigma \\ v_i = v_i^0 \text{ on } \Gamma_v \end{array}\right\} \tag{A.1}$$

Here σ'_{ij} are the deviatoric stress components,

$$\sigma'_{ij} = \sigma_{ij} - \frac{1}{3} \delta_{ij} \sigma_{kk}$$

p is the hydrostatic pressure, f_i the components of body force per unit volume, d_{ij} the components of the deformation rate tensor, v_i the velocity components, μ the viscoscity of the fluid, and S_i and v_i^0 denote prescribed tractions and velocities on portions Γ_σ and Γ_v of the boundary Γ of the domain $\Omega \subset \mathbb{R}^3$ with unit exterior normal $\underset{\sim}{n}$.

We shall momentarily set $\underset{\sim}{f} = \underset{\sim}{0}$, $\underset{\sim}{s} = \underset{\sim}{0}$ without loss in generality.

We next introduce a special complementary energy functional Φ defined on a space of self-equilibrating deviatoric stresses and hydrostatic pressures:

$$\Phi : \Sigma \rightarrow \mathbb{R}$$

$$\Sigma = \{(\underset{\sim}{\sigma}', p) \quad S \times P \mid \sigma'_{ij,j} - p_{,i} = 0 , \tag{A.2}$$

$$(\sigma'_{ij} - p\, \delta_{ij})\, n_j = 0 \quad \text{on} \quad \Gamma_\sigma \}$$

$$\Phi(\underset{\sim}{\sigma}', p) = -\int_\Omega \frac{1}{4\mu} \sigma'_{ij}\, \sigma'_{ij}\, dx + \int_{\Gamma_v} (\sigma_{ij} - p\, \delta_{ij})\, n_j\, v_i^0\, ds \tag{A.3}$$

Here S and P are spaces of stresses and pressures, respectively, defined on the closed body $\bar{\Omega}$ which contain functions sufficiently smooth that the functional Φ is well-defined. The functional Φ is essentially that introduced by Bratineau and Atluri*.

Formally, the Euler-Lagrange equations corresponding to the stationary condition

$$\forall (\bar{\sigma}', \bar{\rho}) : \delta\, \Phi\, (\sigma', \rho) , (\bar{\sigma}', \bar{\rho})) = 0 \tag{A.4}$$

are

$$\left.\begin{aligned} v_{(i,j)} &\equiv d_{ij} = \frac{1}{2\mu} \sigma'_{ij} \\ v_{ii} &= \nabla \cdot \underset{\sim}{v} = 0 \end{aligned}\right\} \tag{A.5}$$

---

*Bratineau, C., Ying, L. A., and Atluri, S. N., "Analysis of Stokes Flow by a Hybrid Method," Finite Element Flow Analysis, University of Tokyo Press, pp. 981-988, 1982.

Our next step is to introduce a perturbation Φ_ε of Φ associated with the hydrostatic pressures p . Let ε denote an arbitrary positive number. Then we define

$$\Phi_\varepsilon(\underset{\sim}{\sigma}', p) = \Phi(\underset{\sim}{\sigma}', p) + \frac{\varepsilon}{2} \int_\Omega p^2 \, dx \tag{A.6}$$

Let

$$\left.\begin{aligned} ||\underset{\sim}{\sigma}'||_0^2 &= \int_\Omega \sigma'_{ij} \sigma'_{ij} \, dx = (\underset{\sim}{\sigma}', \underset{\sim}{\sigma}') \\ ||p||^2 &= \int_\Omega p^2 \, dx \end{aligned}\right\} \tag{A.7}$$

Then, for any fixed $p_0 \in P$, the functional $\underset{\sim}{\sigma}' \to \Phi(\underset{\sim}{\sigma}', p)$ is concave, differentiable, and coercive:

$$\begin{aligned} \Phi_\varepsilon(\underset{\sim}{\sigma}', p_0) &= \frac{1}{4\mu} ||\underset{\sim}{\sigma}'||_0^2 + (\underset{\sim}{\sigma}' \; \underset{\sim}{\nabla} \underset{\sim}{v}) + C(p_0, \underset{\sim}{v}) \\ &\leq \frac{1}{4\mu} ||\underset{\sim}{\sigma}'||_0^2 + ||\underset{\sim}{\sigma}||_0 \; ||\underset{\sim}{\Delta} \underset{\sim}{v}||_0 \\ &\qquad + C(p_0, \underset{\sim}{v}) \end{aligned}$$

i.e.,

$$\Phi_\varepsilon(\underset{\sim}{\sigma}', p_0) \to -\infty \text{ as } ||\sigma'||_0 \to +\infty$$

Likewise, for any fixed $\underset{\sim}{\sigma}'_0 \in S$, the functional $p \to \Phi_\varepsilon(\underset{\sim}{\sigma}'_0, p)$ is concave, differentiable and coercive ($\Phi_\varepsilon(\underset{\sim}{\sigma}'_0, p) \to +\infty$ as $||p|| \to \infty$). Hence, we can conclude that

- *for every* $\varepsilon > 0$, *there exists a unique saddle point* $(\underset{\sim}{\sigma}', p_\varepsilon)$ *of* Φ_ε
- *as* $\varepsilon \to 0$, $(\underset{\sim}{\sigma}'_\varepsilon, p_\varepsilon)$ *conveys to a critical point* $(\underset{\sim}{\sigma}', p)$ *of the functional* Φ .

Notice that $(\underset{\sim}{\sigma}'_\varepsilon , p_\varepsilon)$ satisfies the variational equations

$$\left.\begin{aligned} &\int_\Omega \left(-\frac{1}{2\mu} \sigma'_{ij} + v_{(i,j)}\right) \bar{\sigma}'_{ij} \, dx = 0 \\ &\int_\Omega (-v_{i,i} + \varepsilon p_\varepsilon) \, \bar{p} \, dx = 0 \\ &\qquad\qquad \text{for all } (\underset{\sim}{\bar{\sigma}} , \bar{p}) \in \Sigma \end{aligned}\right\} \tag{A.8}$$

Thus,

$$p_\varepsilon = - \frac{1}{\varepsilon} \operatorname{div} \underset{\sim}{v} \tag{A.9}$$

It appears that the use of Φ_ε is equivalent to appending the complimentary energy with an exterior penalty term corresponding to the incompressibility constraint.

We can relax the constraint $\sigma'_{ij,j} - p,_i = 0$ (equivalently, $(\underset{\sim}{\sigma}', p) \in S \times P$) by introducing the functional,

$$\begin{aligned} &L_\varepsilon : \underset{\sim}{\Lambda} \times S \times P \rightarrow \mathbb{R} \\ &L_\varepsilon (\underset{\sim}{\lambda} , (\underset{\sim}{\sigma}', p)) = \Phi_\varepsilon (\underset{\sim}{\sigma}', p) - + \int_\Omega \lambda_i (\sigma'_{ij,j} - p,_i) \, dx \end{aligned} \tag{A.10}$$

with $\underset{\sim}{\Lambda} = (L^2(\Omega))^3$, the Euler equations of which are (formally),

$$\begin{aligned} -\frac{1}{2\mu} \sigma'_{ij} + v_{(i,j)} &= 0 \\ v_{i,i} &= 0 \\ \sigma'_{ij,j} - p,_i &= 0 \\ \lambda_i - v_i &= 0 \end{aligned}$$

i.e., $\underset{\sim}{\lambda}$ is the velocity field defined on the interior of the domain Ω .

Let us now consider the construction of an assumed-stress hybrid finite element approximation using the functional Φ_ϵ (and ultimately L_ϵ. We begin in the traditional way by introducing approximations of the stress $\tilde{\sigma}'$ and the boundary velocities $\tilde{v}$ form

$$\tilde{\sigma}' = \begin{Bmatrix} \sigma_{11} \\ \sigma_{22} \\ \sigma_{12} \end{Bmatrix} = \tilde{P}(\tilde{x})\tilde{\beta} \tag{A.11}$$

$$\tilde{v} = \begin{Bmatrix} v_1(\tilde{x}) \\ v_2(\tilde{x}) \end{Bmatrix} = \tilde{L}\tilde{q}$$

where $\tilde{P}$ is a matrix of polynomials in local element coordinates x_1, x_2, $\tilde{\beta}$ is a vector of stress parameters, $\tilde{L}$ is a matrix of polynomials in x_1, x_2 and $\tilde{q}$ is a vector of nodal velocities associated with boundary nodes. Likewise, we approximate the element hydrostatic pressure field p by

$$p = \tilde{A}(\tilde{x})\tilde{p} \tag{A.12}$$

where $\tilde{A}$ is, again, a new matrix of polynomials of $\tilde{p}$ is a vector of pressure degrees-of-freedom. At this stage, $\tilde{p}$ and $\tilde{A}$ should be selected so that $\sigma'_{ij,j} - p_{,i}$ (or, in matrix notation, $\tilde{D}^T\tilde{\sigma} - \tilde{\nabla}\,\tilde{p} = 0$).

With these notations, the functional Φ_ϵ for a typical finite element becomes

$$\Phi_\epsilon(\tilde{\beta}, \tilde{p}) = \frac{1}{2}\tilde{\beta}^T\tilde{H}\tilde{\beta} + \tilde{\beta}^T\tilde{T}\tilde{q} - \tilde{p}^T\tilde{Q}\tilde{q} + \frac{\epsilon}{2}\tilde{p}^T\tilde{M}\tilde{p} \tag{A.13}$$

where

$$
\left.
\begin{aligned}
\underset{\sim}{H} &= \frac{1}{2\mu} \int_\Omega \underset{\sim}{P}^T \underset{\sim}{P} \, dx \\
\underset{\sim}{T} &= \int_\Gamma \underset{\sim}{P}^T \underset{\sim}{n} \underset{\sim}{L} \, ds \\
\underset{\sim}{Q} &= \int_\Gamma \underset{\sim}{A}^T \underset{\sim}{n} \underset{\sim}{L} \, ds \\
\underset{\sim}{M} &= \int_\Omega \underset{\sim}{A}^T \underset{\sim}{A} \, dx
\end{aligned}
\right\} \qquad (A.14)
$$

The discrete functional assumes a stationary value whenever

$$
\left.
\begin{aligned}
\frac{\partial \Phi_\varepsilon}{\partial \underset{\sim}{\beta}} = \underset{\sim}{0} & \qquad - \underset{\sim}{H} \underset{\sim}{\beta} + \underset{\sim}{T} \underset{\sim}{q} \\
\frac{\partial \Phi_\varepsilon}{\partial \underset{\sim}{\ }} = \underset{\sim}{0} & \qquad - \underset{\sim}{Q} \underset{\sim}{q} + \varepsilon \underset{\sim}{M} \underset{\sim}{\ }
\end{aligned}
\right\} \qquad (A.15)
$$

Thus

$$\underset{\sim}{\beta} = \underset{\sim}{H}^{-1} \underset{\sim}{T} \underset{\sim}{q} \qquad (A.16)$$

$$\underset{\sim}{\ } = \frac{1}{\varepsilon} \underset{\sim}{M}^{-1} \underset{\sim}{Q} \underset{\sim}{q} \qquad (A.17)$$

and, therefore,

$$\Phi_\varepsilon = \frac{1}{2} \underset{\sim}{q}^T \underset{\sim}{K}_\varepsilon \underset{\sim}{q} \qquad (A.18)$$

where $\underset{\sim}{K}_\varepsilon$ is the perturbed stiffness matrix,

$$\underset{\sim}{K}_\varepsilon = \underset{\sim}{T}^T \underset{\sim}{H}^{-1} \underset{\sim}{T} - \frac{1}{\varepsilon} \underset{\sim}{Q}^T \underset{\sim}{M}^{-1} \underset{\sim}{Q} \qquad (A.19)$$

The matrix $\underset{\sim}{T}^T \underset{\sim}{H}^{-1} \underset{\sim}{T}$ is the usual assumed-stress hybrid stiffness matrix for the element whereas $-\underset{\sim}{Q}^T \underset{\sim}{M}^{-1} \underset{\sim}{Q}$ is a penalty-type matrix associated with the constraint $\text{div}\, \underset{\sim}{v} = 0$. Notice that the hydrostatic pressure has been eliminated completely from the formulation, and is computed a posteriori by the formula

$$\underset{\sim}{\rho} = \underset{\sim}{A}\,\underset{\sim}{\rho} = \frac{1}{\epsilon}\,\underset{\sim}{A}\,\underset{\sim}{M}^{-1}\,\underset{\sim}{Q}\,\underset{\sim}{q} \tag{A.20}$$

Interior Velocity Formulation. An enriched approximation, which may lead to coordinate-invariant stiffness matrices, is obtained if we repeat the above calculations using the perturbed Lagrangian L_ϵ of (A.10). This necessitates that we introduce an independent approximation of the interior velocity $\lambda = \underset{\sim}{V}$ of the type

$$\underset{\sim}{\lambda} = \begin{Bmatrix} \lambda_1 \\ \lambda_2 \end{Bmatrix} = \underset{\sim}{b}\,\underset{\sim}{\mu} \tag{A.21}$$

where $\underset{\sim}{b}$ is a matrix of "bubble functions" (generally vanishing on Γ) associated with degree-of-freedom parameters $\underset{\sim}{\mu}$. For a typical element, we have,

$$L_\epsilon = \Phi_\epsilon(\underset{\sim}{\beta}, \underset{\sim}{p}) + \underset{\sim}{\mu}^T \underset{\sim}{B}\,\underset{\sim}{\beta} - \underset{\sim}{\mu}^T \underset{\sim}{C}\,\underset{\sim}{p}$$

wherein $\Phi_\epsilon(\underset{\sim}{\beta}, \underset{\sim}{p})$ is given by (13) and

$$\left.\begin{aligned} \underset{\sim}{B} &= \int_\Omega \underset{\sim}{b}^T \underset{\sim}{D}^T \underset{\sim}{P}\,dx \\ \underset{\sim}{C} &= \int_\Omega \underset{\sim}{b}^T \underset{\sim}{\nabla}^T \underset{\sim}{A}\,dx \end{aligned}\right\} \tag{A.22}$$

Thus, instead of (15) we have

$$\left.\begin{aligned} -\underset{\sim}{H}\,\underset{\sim}{\beta} + \underset{\sim}{T}\,\underset{\sim}{q} + \underset{\sim}{B}^T \underset{\sim}{\mu} &= \underset{\sim}{0} \\ -\underset{\sim}{Q}\,\underset{\sim}{q} + \epsilon\,\underset{\sim}{M}\,\underset{\sim}{p} - \underset{\sim}{C}^T \underset{\sim}{\mu} &= \underset{\sim}{0} \\ \underset{\sim}{B}\,\underset{\sim}{\beta} - \underset{\sim}{C}\,\underset{\sim}{p} &= \underset{\sim}{0} \end{aligned}\right\} \tag{A.23}$$

from which we compute

$$\underset{\sim}{\mu} = \underset{\sim}{S}_0 \underset{\sim}{q} - \frac{1}{\varepsilon} \underset{\sim}{S}_1 \underset{\sim}{q} \tag{A.24}$$

where

$$\left.\begin{aligned} \underset{\sim}{S}_0 &= \underset{\sim}{R}_\varepsilon^{-1} \underset{\sim}{B} \underset{\sim}{H}^{-1} \underset{\sim}{T} \\ \underset{\sim}{S}_1 &= \underset{\sim}{R}_\varepsilon^{-1} \underset{\sim}{c} \underset{\sim}{M}^{-1} \underset{\sim}{Q} \\ \underset{\sim}{R}_\varepsilon &= \underset{\sim}{B} \underset{\sim}{H}^{-1} \underset{\sim}{B}^T + \frac{1}{\varepsilon} \underset{\sim}{c} \underset{\sim}{M}^{-1} \underset{\sim}{c}^T \end{aligned}\right\} \tag{A.25}$$

Hence,

$$\left.\begin{aligned} \underset{\sim}{\beta} &= \underset{\sim}{H}^{-1} (\underset{\sim}{T} + \underset{\sim}{B}^T \underset{\sim}{S}) \underset{\sim}{q} \\ \underset{\sim}{p} &= \frac{1}{\varepsilon} \underset{\sim}{M}^{-1} (\underset{\sim}{Q} + \underset{\sim}{c}^T \underset{\sim}{S}) \underset{\sim}{q} \end{aligned}\right\} \tag{A.26}$$

with $\underset{\sim}{S} = \underset{\sim}{S}_0 - \varepsilon^{-1} \underset{\sim}{S}_1$. Finally, the element stiffness matrix is

$$\begin{aligned} \underset{\sim}{K}_\varepsilon = (\underset{\sim}{T} + \underset{\sim}{B}^T \underset{\sim}{S})^T \underset{\sim}{H}^{-1} (\underset{\sim}{T} + \underset{\sim}{B}^T \underset{\sim}{S}) - \varepsilon^{-1} (\underset{\sim}{Q} + \underset{\sim}{c}^T \underset{\sim}{S})^T \\ \underset{\sim}{M}^{-1} (\underset{\sim}{Q} + \underset{\sim}{c}^T \underset{\sim}{S}) \end{aligned} \tag{A.27}$$

and the hydrostatic pressure is given by

$$P = \frac{1}{\varepsilon} \underset{\sim}{A} \underset{\sim}{p} \tag{A.28}$$

where $\underset{\sim}{p}$ is defined in (A.26).

Appendix B

SPAR USER'S MANUAL UPDATES

Appendix B

Included as an attachment to this appendix are update pages to the SPAR Structural Analysis System Reference Manual (NASA CR 158970-1) dated December 1978. These updates describe the use of a new processor, EKSF, used to generate element intrinsic stiffness matrices for incompressible viscous flow analyses. Also described is the velocity vector version of PLTB, PLTB/VVEC, used for plotting flow vectors indicating the magnitude and direction of velocities.

Attachment to Appendix B

Update pages to the SPAR Structural Analysis System
Reference Manual (NASA CR 158970-1)

Section

PRECEDING PAGE BLANK NOT FILMED

Table 1-2: SPAR PROCESSOR FUNCTIONS

NAME AND SECTION REFERENCE		FUNCTION
TAB	3.1	Translates user inputs into data sets containing basic tables of information such as: - Joint Locations - Material Constants - Element Section Properties - Joint Reference Frame Orientations - Constraint Conditions - Rigid Lumped Mass Data (See Section 3.1 for a complex list)
ELD	3.2	Produces data sets containing basic element definitions, i.e., connected joints, integers pointing to applicable lines in tables of section properties, material constants, etc.
E	3.3	Generates a system of data sets called the 'E-state,' consisting of individual element information packets containing data such as element geometry (dimensions, orientation), and literal section properties. E also forms the system diagonal mass matrix.
EKS	3.4	Computes element stiffness and stress influence matrices, and inserts them into the 'E-state.'
EKSF	3.5	Computes incompressible viscous flow "stiffness" matrices and inserts them into the 'E-state.'
TOPO	4.1	Analyzes element interconnection topology, and produces data sets used to guide other SPAR processors in forming and factoring assembled system matrices.
K	4.2	Forms system elastic stiffness matrix.
M	4.3	Forms system consistent mass matrix.
KG	4.4	Forms system geometric (pre-stress) stiffness matrix.
FSM	12	Forms system matrices (dilitational strain energy, gravitational energy, kinetic energy) associated with fluid elements.
INV	4.5	Factors system matrices in SPAR's standard sparse-matrix format, e.g., K, K+KG, K-CM.

Section 3

STRUCTURE DEFINITION

To define the basic finite element model of the structure, the user proceeds as follows.

- Execute TAB to define joint locations, joint reference frame orientations, tables of section properties, and other basic components of the problem definition, as summarized on Table TAB-1 in Section 3.1.

- Execute AUS/TABLE to generate tables of section properties for three-dimensional solid and fluid elements, if required, as decribed in Section 3.2.2.3.

- Execute ELD to generate data sets containing basic element definitions, i.e., connected joints, integers pointing to applicable lines in tables of section properties, etc.

- Execute E to generate a system of data sets called the "E-state," consisting of individual element information packets containing data such as element geometry (dimensions, orientation), and literal section properties.

- E also produces the system diagonal mass matrix.

- EKS is executed to compute individual element stiffness and stress recovery matrices, and insert them into the E-state.

or

- EKSF is executed to compute individual element incompressible viscous flow intrinsic "stiffness" matrices, and insert them into the E-state.

All of the basic structural definition data sets produced as outlined above should be retained in Library 1.

Table 1-1: SPAR ELEMENT REPERTOIRE

Name	Description	See Volume 1 Sections:
E21	General straight beam elements such as such as channels, wide-flanges, angles, tubes, zees, etc.	3.1.7 - 9
E22	Beams for which the intrinsic stiffness matrix is given	3.1.10
E23	Bar - Axial Stiffness only	3.1.11
E24	Plane Beam	3.1.12
E25	Zero-Length Element Used to Elastically Connect Geometrically Coincident Joints	3.1.10
	Two-Dimensional (area) Elements	3.1.13
E31	Triangular Membrane	
E32	Triangular Plate	
E33	Triangular Combined Membrane and Bending Element	
E41	Quadrilateral Membrane, or 2-D Incompressible Viscous Flow Element (when used with EKSF).	
E42	Quadrilateral Plate	
E43	Quadrilateral Combined Membrane and Bending Element	
E44	Quadrilateral Shear Panel	3.1.14
	Three-Dimensional Solids	3.2.2.3
S41	Tetrahedron (Pyramid)	
S61	Pentahedron (Wedge)	
S81	Hexahedron (Brick)	
	Compressible Fluid Elements:	12., 3.2.2.3
F41	Tetrahedron (Pyramid)	
F61	Pentahedron (Wedge)	
F81	Hexahedron (Brick)	

Notes:

- See Section 7.2 for examples of stress output
- See Volume 2 (theory) for element formulation details
- Aeolotropic constitutive relations permitted, all area elements
- Laminated cross sections permitted for E33, E43
- Membrane/bending coupling permitted for E33, E43
- E41, E42, E43, E44 may be warped
- Aeolotropic constitutive relations permitted for 3-D solids
- Non-structural mass permitted for line and area elements.

3.5 EKSF-INCOMPRESSIBLE VISCOUS FLOW ELEMENT INTRINSIC STIFFNESS MATRIX GENERATOR

Function. EKSF functions similarly to EKS, i.e., based on the dimensions, section properties, etc., currently embedded in the element information packets originated by processor E, EKSF computes intrinsic stiffness and stress matrices for all elements other than E41 elements (e.g., E21 elements) and inserts them into the packets. For E41 elements, EKSF computes incompressible viscous flow "stiffness" matrices and inserts them into the packets.

RESET Controls. Two additional reset controls have been incorporated into EKSF which apply to E41 elements only.

RESET Controls

Name	Default Value	Meaning
ELIB	1	Library containing the element information packets.
TIME	0	Nonzero value causes printout of intermediate CP and wall clock times.
GAZERO	$10.^{-20}$	Zero-test parameter, (beam area) x (shear modulus).
CIZERO	$10.^{-20}$	Zero-test parameter, beam non-uniform torsion constant.
EPSILN	.001	The penalty parameter, ε, used to enforce incompressibility.
XMU	$10.^{-4}$	Shear viscosity of the fluid.

Note: EPSILN and XMU apply to E41 elements only.

Core Requirements. EKS requires only a buffer area through which element information packets are transmitted. About 5,000 - 15,000 locations are usually suitable. IO counts will vary in inverse proportion to core space.

Velocity Vector Version (PLTB/VVEC)

PLTB/VVEC functions like PLTB except that for all "deformed" plots, the "displacements" (flow velocities when executing in the viscous flow mode) are plotted with arrows indicating the magnitude and direction of the joint "displacements." The control statement DNORM remains in effect for normalizing joint "displacements" (velocities). Options 24 and 25 do not apply to this processor. All "deformations" are plotted as flow vectors. (See examples in Appendix.)

Note: PLTB/VVEC is available for plotting on the FR-80 plotter only.

Appendix C

PARALLEL FLOW IN A STRAIGHT CHANNEL
MODEL PROBLEM A

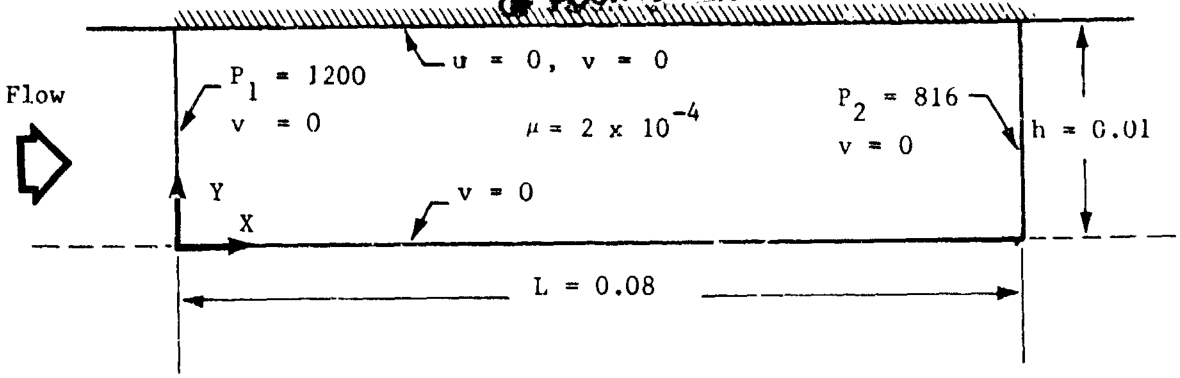

a. Domain and Boundary Condition Definitions

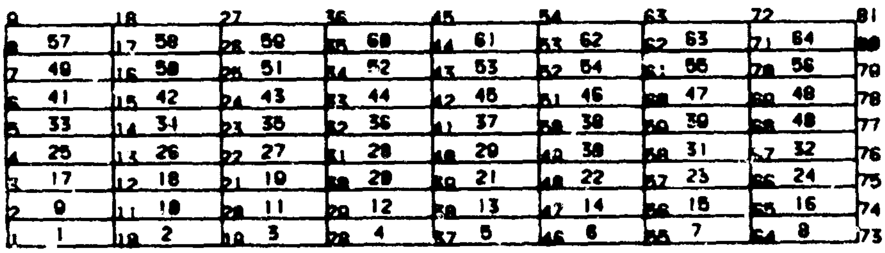

b. Finite Element Mesh

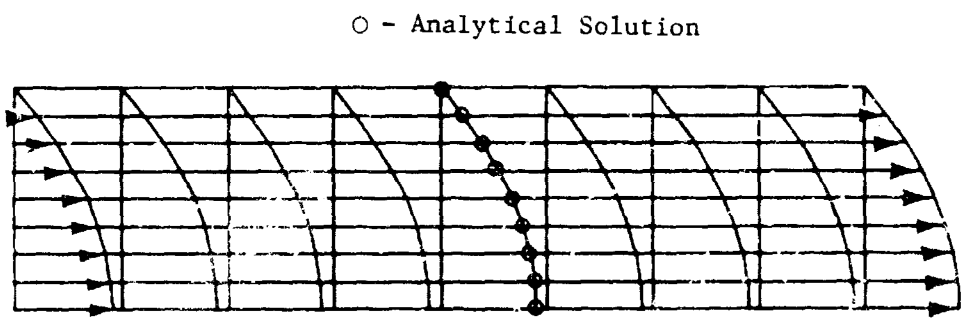

c. Calculated Velocity Field

Fig. C-1 - Parallel Flow in a Straight Channel

Table C-1

INPUT DATA FOR MODEL PROBLEM A

```
PEARSNBIN202*SPAR(1).TESTA2/R
      @XQT TAB
      START 81    3 4 5 6     $  2-D , NO ROTATIONS
      TITLE' MODEL PROBLEM A
       MATC
        1    30.+06   .33
       JLOC
        1    0.    0.    0.    0.    .01    0.    9    1    9
        9   .08    0.    0.   .08    .01    0.
       SA
        1    1.0
       CON=1
      ZERO    1,2: 9,81,9
      ZERO       2: 1,73,9: 2,8: 74,80
      @XQT ELD
       E41
         1    10    11    2    1    8    8
      @XQT E
      @XQT EKSF
       RESET XMU=2.-04
      @PMD,E
      @XQT TOPO
      @XQT K
      RESET SPDP 2
      @XQT INV
      @XQT AUS
       SYSVEC
       APPLIED FORCES
       CASE 1
       I=1: J=2,8: 1.5
       I=1: J=1: .75
       I=1: J=74,80: 1.02
       I=1: J=73: 0.51
      @XQT SSOL
      @XQT VPRT
       PRINT STAT REAC 1 1
       PRINT STAT DISP 1 1
      @XQT DCU
       TOC 1
```

Table C-2

COMPUTED VELOCITIES FOR MODEL PROBLEM A

STATIC DISPLACEMENTS.

JOINT	1	2
1	.316+04	.000 *
2	.311+04	.000 *
3	.296+04	.000 *
4	.271+04	.000 *
5	.236+04	.000 *
6	.191+04	.000 *
7	.137+04	.000 *
8	.732+03	.000 *
9	.000 *	.000 *
10	.315+04	.000 *
11	.310+04	.230+01
12	.295+04	.394+01
13	.270+04	.461+01
14	.236+04	.444+01
15	.192+04	.347+01
16	.138+04	.210+01
17	.738+03	.710+00
18	.000 *	.000 *
19	.315+04	.000 *
20	.310+04	-.192+01
21	.295+04	-.318+01
22	.270+04	-.363+01
23	.236+04	-.353+01
24	.192+04	-.277+01
25	.138+04	-.175+01
26	.738+03	-.664+00
27	.000 *	.000 *
28	.315+04	.000 *
29	.310+04	.117+01
30	.295+04	.192+01
31	.270+04	.225+01
32	.236+04	.242+01
33	.192+04	.199+01
34	.138+04	.137+01
35	.738+03	.600+00
36	.000 *	.000 *
37	.314+04	.000 *
38	.309+04	.294+00
39	.295+04	.483+00
40	.270+04	.353+00
41	.236+04	-.305+00
42	.192+04	-.578+00
43	.138+04	-.664+00
44	.739+03	-.436+00
45	.000 *	.000 *
46	.315+04	.000 *
47	.310+04	-.986+00
48	.295+04	-.161+01
49	.270+04	-.158+01
50	.236+04	-.730+00

(Continued)

Table C-2 (Concluded)

51	.192+04	-.112+00
52	.138+04	.307+00
53	.738+03	.336+00
54	.000 *	.000 *
55	.315+04	.000 *
56	.310+04	.279+00
57	.295+04	.376+00
58	270+04	.147+00
59	.236+04	-.514+00
60	.192+04	-.805+00
61	.138+04	-.783+00
62	.737+03	-.434+00
63	.000 *	.000 *
64	.315+04	.000 *
65	.310+04	.467+00
66	.295+04	.895+00
67	.271+04	.127+01
68	.236+04	.162+01
69	.192+04	.153+01
70	.138+04	.109+01
71	.737+03	.444+00
72	.000 *	.000 *
73	.314+04	.000 *
74	.309+04	.000 *
75	.295+04	.000 *
76	.270+04	.000 *
77	.236+04	.000 *
78	.192+04	.000 *
79	.138+04	.000 *
80	.741+03	.000 *
81	.000 *	.000 *

EXIT 2.792 0 6

C-2

Appendix D

PLANE SLIDER BEARING MODEL PROBLEM B

ORIGINAL PAGE IS OF POOR QUALITY

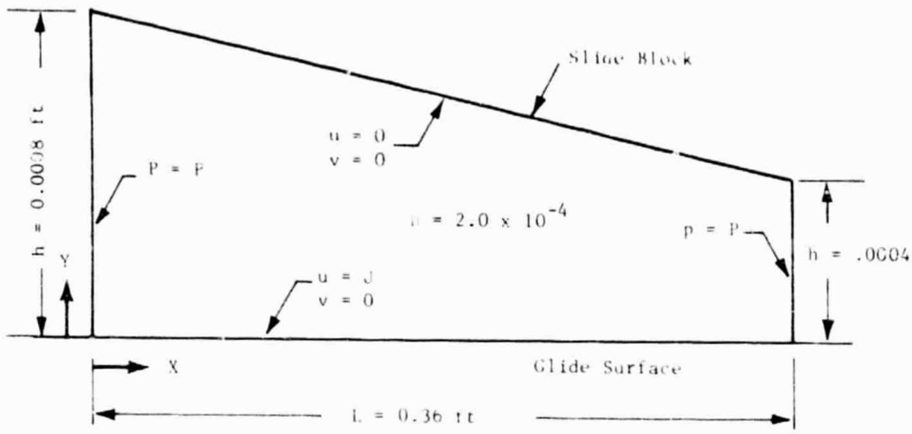

a. Domain and Boundary Condition Definitions

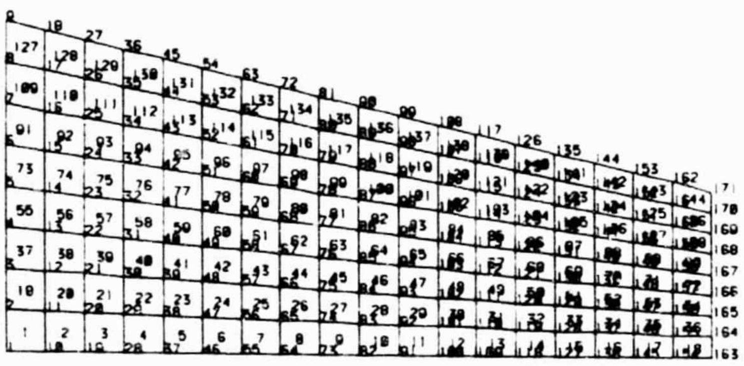

b. Finite Element Mesh

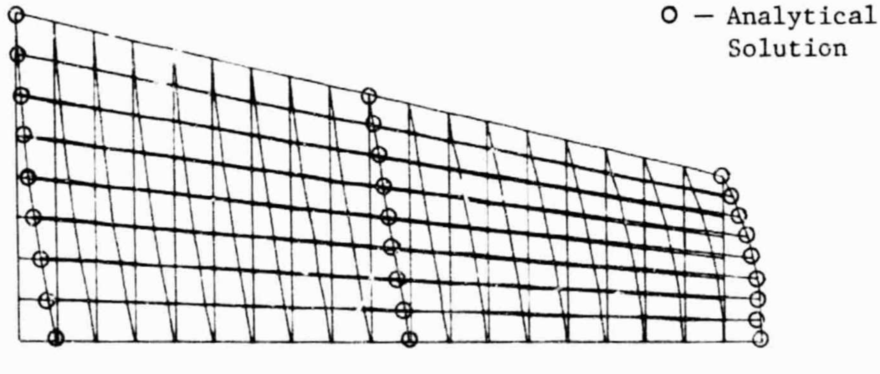

c. Calculated Velocity Field

Fig. D-1 - Plane Slider Bearing

Table D-1

INPUT DATA FOR MODEL PROBLEM B

```
PEARSNBIN202*SPAR(1).TESTB/R
        @XQT TAB
        START 171   3 4 5 6    $  2-D , NO ROTATIONS
        TITLE' MODEL PROBLEM B
         MATC
          1   30.+06   .33
         JLOC
          1   0.   0.   0.   0.   .0006   0.   9  1  19
          9   .36   0.   0.   .36   .0004   0.
         SA
          1   1.0
         CON=1
         ZERO  1,2: 9,171,9
         ZERO     2: 1,163,9
         NONZERO  1: 1,163,9
        @XQT ELD
         E41
          1  10  11  2  1  18  8
        @XQT E
        @XQT EKSF
         RESET XMU=2.-04
        @XQT TOPO
        @XQT K
         RESET SPDP 2
        @XQT INV
        @XQT AUS
         SYSVEC
         APPLIED FORCES
         CASE 1
         I=1: J=2,8:1.0
         I=1: J=164,170: 0.5
         SYSVEC
        APPLIED MOTION
        CASE 1
        I=1: J=1,163,9: 100.0
        @XQT SSOL
        @XQT VPRT
         PRINT STAT REAC 1 1
         PRINT STAT DISP 1 1
        @XQT DCU
         TOC 1
```

ORIGINAL PAGE IS
OF POOR QUALITY

Table D-2

COMPUTED VELOCITIES FOR MODEL PROBLEM B

STATIC DISPLACEMENTS.

JOINT	1	2
1	.100+03*	.000 *
2	.781+02	-.179+00
3	.622+02	-.355+00
4	.460+02	-.413+00
5	.332+02	-.464+00
6	.225+02	-.401+00
7	.125+02	-.335+00
8	.726+01	-.163+00
9	.000 *	.000 *
10	.100+03*	.000 *
11	.828+02	.156+00
12	.636+02	.307+00
13	.488+02	.354+00
14	.346+02	.395+00
15	.223+02	.339+00
16	.133+02	.283+00
17	.363+01	.136+00
18	.000 *	.000 *
19	.100+03*	.000 *
20	.793+02	-.139+00
21	.643+02	-.271+00
22	.486+02	-.313+00
23	.360+02	-.350+00
24	.251+02	-.302+00
25	.146+02	-.252+00
26	.846+01	-.123+00
27	.000 *	.000 *
28	.100+03*	.000 *
29	.840+02	.117+00
30	.657+02	.225+00
31	.514+02	.255+00
32	.374+02	.263+00
33	.250+02	.241+00
34	.155+02	.200+00
35	.491+01	.953-01
36	.000 *	.000 *
37	.100+03*	.000 *
38	.806+02	-.101+00
39	.666+02	-.195+00
40	.514+02	-.222+00
41	.389+02	-.246+00
42	.278+02	-.212+00
43	.167+02	-.176+00
44	.971+01	-.861-01
45	.000 *	.000 *
46	.100+03*	.000 *
47	.853+02	.803-01
48	.679+02	.151+00
49	.543+02	.166+00
50	.405+02	.181+00

(Continued)

Table D-2 (Continued)

51	.279+02	.151+00	76	.579+02	-.671-01
52	.178+02	.124+00	77	.458+02	-.693-01
53	.629+01	.574-01	78	.342+02	-.573-01
54	.000 *	.000 *	79	.218+02	-.444-01
55	.100+03*	.000 *	80	.127+02	-.210-01
56	.821+02	-.673-01	81	.000 *	.000 *
57	.691+02	-.126+00	82	.100+03*	.000 *
58	.545+02	-.140+00	83	.885+02	.165-01
59	.421+02	-.153+00	84	.733+02	.220-01
60	.308+02	-.130+00	85	.611+02	.139-01
61	.191+02	.107+00	86	.478+02	.512-02
62	.111+02	-.521-01	87	.348+02	-.501-02
63	.000 *	.000 *	88	.234+02	-.111-01
64	.100+03*	.000 *	89	.953+01	-.109-01
65	.868+02	.470-01	90	.000 *	.000 *
66	.704+02	.834-01	91	.100+03*	.000 *
67	.575+02	.865-01	92	.856+02	-.719-02
68	.439+02	.891-01	93	.750+02	-.584-02
69	.311+02	.697-01	94	.618+02	-.757-03
70	.204+02	.538-01	95	.499+02	.670-02
71	.781+01	.221-01	96	.381+02	.924-02
72	.000 *	.000 *	97	.250+02	.130-01
73	.100+03*	.000 *	98	.145+02	.731-02
74	.837+02	-.360-01	99	.000 *	.000 *
75	.718+02	-.630-01	100	.100+03*	.000 *

(Continued)

Table D-2 (Continued)

101	.905+02	-.115-01	126	.000 *	.000 *
102	.768+02	-.344-01	127	.100+03*	.000 *
103	.654+02	-.529-01	128	.905+02	.438-01
104	.524+02	-.727-01	129	.834+02	.950-01
105	.391+02	-.747-01	130	.723+02	.116+00
106	.268+02	-.719-01	131	.611+02	.141+00
107	.115+02	-.420-01	132	.486+02	.126+00
108	.000 *	.000 *	133	.334+02	.113+00
109	.100+03*	.000 *	134	.194+02	.562-01
110	.878+02	.193-01	135	.000 *	.000 *
111	.787+02	.466-01	136	.100+03*	.000 *
112	.665+02	.600-01	137	.959+02	-.610-01
113	.549+02	.764-01	138	.862+02	-.135+00
114	.428+02	.762-01	139	.772+02	-.174+00
115	.287+02	.655-01	140	.649+02	-.215+00
116	.167+02	.331-01	141	.508+02	-.203+00
117	.000 *	.000 *	142	.361+02	-.184+00
118	.100+03*	.000 *	143	.170+02	-.998-01
119	.929+02	-.373-01	144	.000 *	.000 *
120	.809+02	-.567-01	145	.100+03*	.000 *
121	.706+02	-.115+00	146	.939+02	.664-01
122	.580+02	-.1[illegible]6+00	147	.893+02	.139+00
123	.443+02	-.141+00	148	.797+02	.167+00
124	.309+02	-.129+00	149	.691+02	.199+00
125	.139+02	-.715-01	150	.561+02	.176+00

(Continued)

Table D-2 (Concluded)

151	.394+02	.156+00
152	.229+02	.765-01
153	.000 *	.000 *
154	.100+03*	.000 *
155	.100+03	-.827-01
156	.930+02	-.180+00
157	.857+02	-.229+00
158	.741+02	-.260+00
159	.594+02	-.263+00
160	.430+02	-.237+00
161	.209+02	-.127+00
162	.000 *	.000 *
163	.100+03*	.000 *
164	.986+02	.868-01
165	.973+02	.179+00
166	.897+02	.213+00
167	.797+02	.250+00
168	.660+02	.220+00
169	.473+02	.193+00
170	.276+02	.932-01
171	.000 *	.000 *

EXIT 9.477 0 6

Appendix E

DRIVEN CAVITY FLOW
MODEL PROBLEM C

1 x 1 Box $\mu = 0.1$

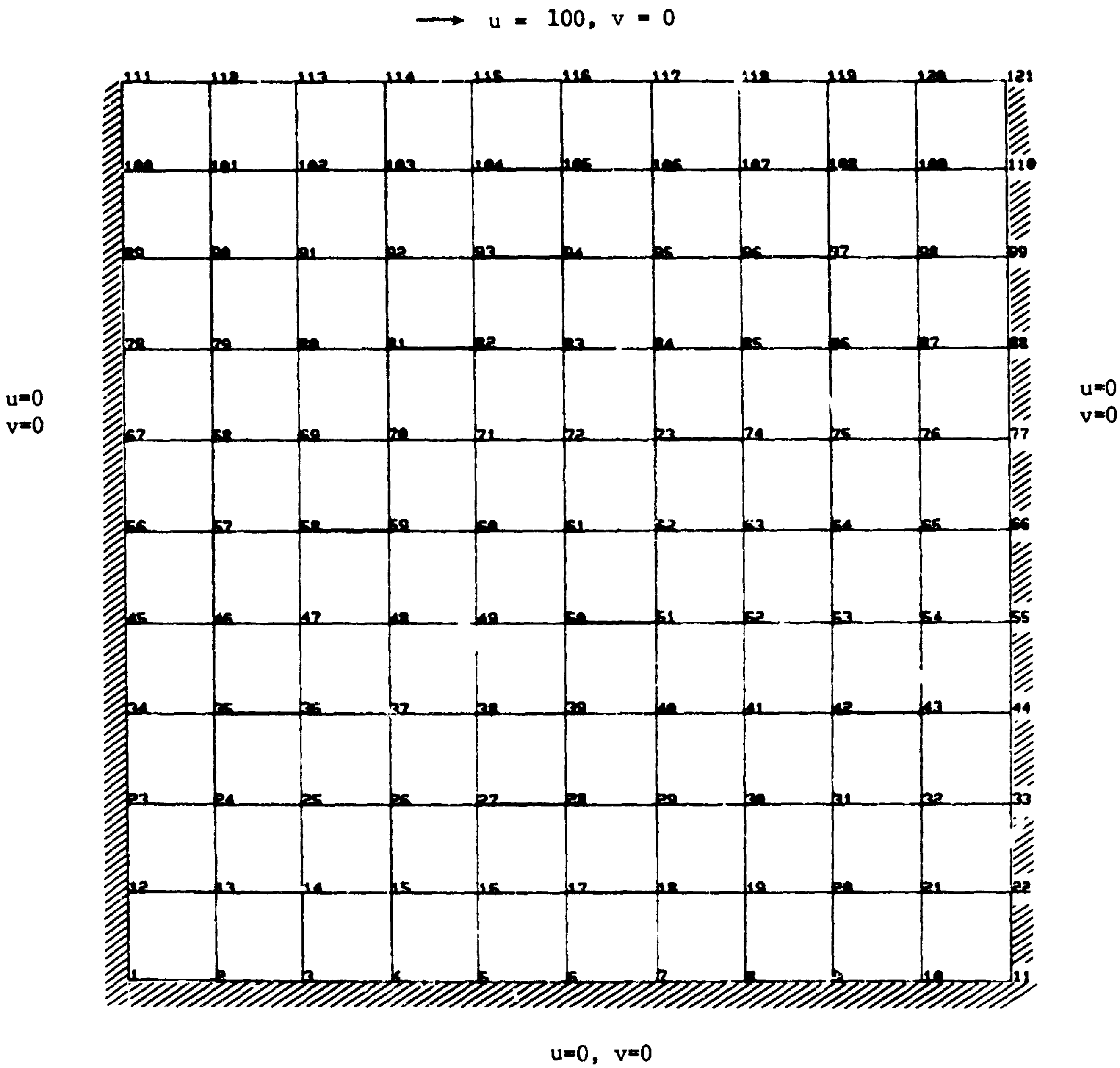

Fig. E-1 - Driven Cavity Problem
Finite Element Mesh and Boundary Conditions

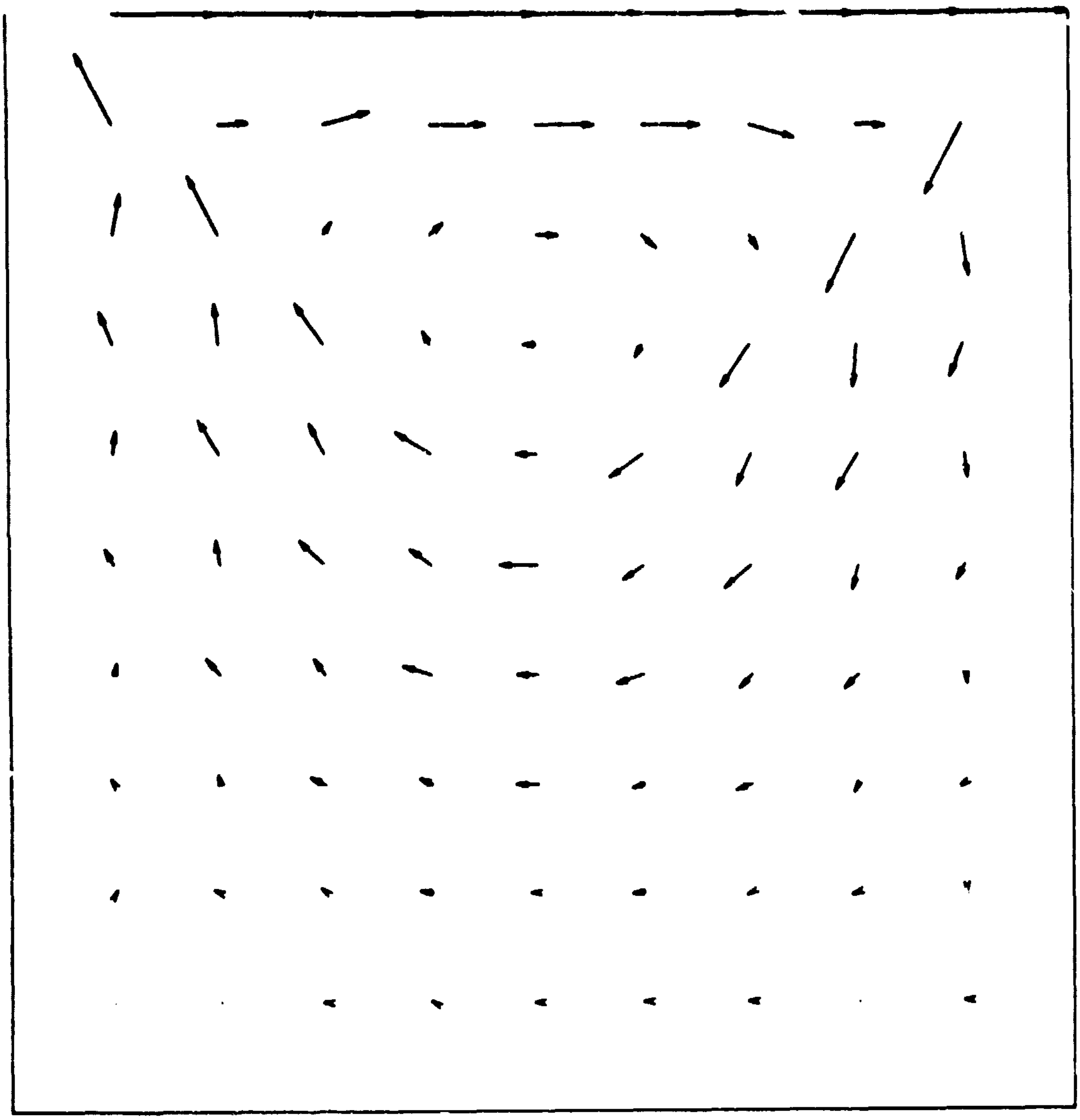

Fig. E-2 - Driven Cavity Problem
Computed Velocity Field

Table E-1

INPUT DATA FOR MODEL PROBLEM C

```
PEARSNDIN202*SPAR(1).TESTC/R
        @XQT TAB
        START 121   3 4 5 6    $  2-D , NO ROTATIONS
        TITLE' MODEL PROBLEM C
         MATC
          1   30.+06   .33
         JLOC
          1   0.    0.    0.    1.0    0.    0.    11    1    11
         11   0.    1.0   0.    1.0    1.0   0.
         SA
          1   1.0
         CON=1
         ZERO    1,2: 1,111,11
         ZERO    1,2: 11,121,11
         ZERO    1,2: 2,10
         ZERO      2: 112,120
         NONZERO   1: 112,120
        @XQT ELD
         E41
           1    2    13    12     1    10    10
        @XQT E
        @XQT EKSF
         RESET XHU=.1
        @PMD,E
        @XQT TOPO
        @XQT K
        RESET SPOP 2
        @XQT INV
        @XQT AUS
         SYSVEC
         APPLIED MOTIONS
         CASE 1
         I=1: J=112,120: 100.0
        @XQT SSOL
        @XQT VPRT
         PRINT STAT REAC 1 1
         PRINT STAT DISP 1 1
        @XQT DCU
         TOC 1
```

Table E-2

COMPUTED VELOCITIES FOR MODEL PROBLEM C

STATIC DISPLACEMENTS.

JOINT	1		2	
1	.000	*	.000	*
2	.000	*	.000	*
3	.000	*	.000	*
4	.000	*	.000	*
5	.000	*	.000	*
6	.000	*	.000	*
7	.000	*	.000	*
8	.000	*	.000	*
9	.000	*	.000	*
10	.000	*	.000	*
11	.000	*	.000	*
12	.000	*	.000	*
13	-.179+01		-.215+00	
14	-.951+00		.138+01	
15	-.453+01		.202+00	
16	-.330+01		.568+00	
17	-.584+01		-.337-01	
18	-.326+01		-.546+00	
19	-.448+01		-.235+00	
20	-.901+00		-.134+01	
21	-.178+01		.218+00	
22	.000	*	.000	*
23	.000	*	.000	*
24	.539+00		.303+01	
25	-.662+01		.246+01	
26	-.524+01		.332+01	
27	-.123+02		.126+01	
28	-.844+01		-.259-01	
29	-.122+02		-.136+01	
30	-.512+01		-.328+01	
31	-.657+01		-.242+01	
32	.588+00		-.297+01	
33	.000	*	.000	*
34	.000	*	.000	*
35	-.447+01		.496+01	
36	-.320+01		.843+01	
37	-.156+02		.641+01	
38	-.127+02		.426+01	
39	-.215+02		-.972-01	
40	-.126+02		-.439+01	
41	-.156+02		-.639+01	
42	-.309+01		-.834+01	
43	-.446+01		-.484+01	
44	.000	*	.000	*
45	.000	*	.000	*
46	.113+01		.103+02	
47	-.129+02		.138+02	
48	-.114+02		.140+02	
49	-.275+02		.779+01	
50	-.202+02		-.107+00	

(Continued)

Table E-2 (Continued)

51	-.275+02	-.795+01	76	.247+01	-.214+02
52	-.113+02	-.141+02	77	.000 *	.000 *
53	-.128+02	-.137+02	78	.000 *	.000 *
54	.117+01	-.101+02	79	-.125+02	.296+02
55	.000 *	.000 *	80	-.351+01	.380+02
56	.000 *	.000 *	81	-.269+02	.384+02
57	-.739+01	.146+02	82	-.719+01	.120+02
58	-.444+01	.226+02	83	-.127+02	.247-01
59	-.247+02	.220+02	84	-.749+01	-.121+02
60	-.208+02	.140+02	85	-.270+02	-.384+02
61	-.363+02	-.722-01	86	-.361+01	-.381+02
62	-.208+02	-.142+02	87	-.126+02	-.296+02
63	-.247+02	-.221+02	88	.000 *	.000 *
64	-.450+01	-.224+02	89	.000 *	.000 *
65	-.745+01	-.144+02	90	.622+01	.380+02
66	.000 *	.000 *	91	-.283+02	.532+02
67	.000 *	.000 *	92	.786+01	.124+02
68	.243+01	.215+02	93	.126+02	.115+02
69	-.188+02	.319+02	94	.205+02	.111+00
70	-.129+02	.291+02	95	.126+02	-.114+02
71	-.319+02	.201+02	96	.776+01	-.126+02
72	-.205+02	-.144+00	97	-.283+02	-.533+02
73	-.320+02	-.202+02	98	.630+01	-.379+02
74	-.132+02	-.290+02	99	.000 *	.000 *
75	-.189+02	-.319+02	100	.000 *	.000 *

(Continued)

Table E-2 (Concluded)

101	-.341+02		.639+02	
102	.287+02		.999+00	
103	.435+02		.117+02	
104	.531+02		-.149+00	
105	.549+02		.123-01	
106	.532+02		.232+00	
107	.436+02		-.119+02	
108	.287+02		-.107+01	
109	-.342+02		-.638+02	
110	.000	*	.000	*
111	.000	*	.000	*
112	.100+03	*	.000	*
113	.100+03	*	.000	*
114	.100+03	*	.000	*
115	.100+03	*	.000	*
116	.100+03	*	.000	*
117	.100+03	*	.000	*
118	.100+03	*	.000	*
119	.100+03	*	.000	*
120	.100+03	*	.000	*
121	.000	*	.000	*

EXIT 13.996 0 6